PHYSICAL REVIEW A VOLUME 43, NUMBER 12 15 JUNE 1991

Cooperative dynamics in visual processing

H. Sompolinsky and D. Golomb
*Racah Institute of Physics, Hebrew University, Jerusalem 91904, Israel**
and AT&T Bell Laboratories, Murray Hill, New Jersey 07974

D. Kleinfeld[†]
AT&T Bell Laboratories, Murray Hill, New Jersey 07974

(Received 24 July 1990; revised manuscript received 6 February 1991)

An oscillator neural network model that is capable of processing local and global attributes of sensory input is proposed and analyzed. Local features in the input are encoded in the average firing rate of the neurons while the relationships between these features can modulate the temporal structure of the neuronal output. Neurons that share the same receptive field interact via relatively strong feedback connections, while neurons with different fields interact via specific, relatively weak connections. The model is studied in the context of processing visual stimuli that are coded for orientation. The effect of axonal propagation delays on synchronization of oscillatory activity is analyzed. We compare our theoretical results with recent experimental evidence on coherent oscillatory activity in the cat visual cortex. The computational capabilities of the model for performing discrimination and segmentation tasks are demonstrated. Coding and linking of visual features other than orientation are discussed.

I. INTRODUCTION

The linking of sensory inputs across multiple receptive fields is a fundamental task of sensory processing.[1–3] Such linkage is necessary to identify distinct objects, segment them from each other, and separate them from background. The theoretical issues raised by this processing have been difficult to approach within the framework of most current neural-network models. This difficulty originates from using only the levels of activity in individual neurons to encode information. It has been suggested by von der Malsburg and Schneider[1] that global properties of stimuli are identified through correlations in the temporal firing patterns of different neurons. This concept gained support from a recent series of experiments by Eckhorn and co-workers[4] and Gray, Singer, and co-workers,[5–8] who showed that neurons in the cat primary visual cortex can exhibit oscillatory responses that are coherent over relatively large distances, and are sensitive to global properties of stimuli.

Before describing the model, we summarize the current status of experimental results that are relevant to our work[4–8] (Fig. 1).

(i) Neurons that respond to moving, oriented bars have a periodic component in their spiking output. The average period, approximately 20–30 ms, appears to be the same for different neurons and is independent of the orientation of the stimulus.

(ii) The activity of neurons with overlapping receptive fields can be synchronized by the presentation of a single, oriented bar. The synchronization is fairly insensitive to the orientation preferences of the neurons [Fig. 1(a)].

(iii) Neurons with separate receptive fields will fire in synchrony *only* if bars that simultaneously pass through the individual fields have similar orientation. Interestingly, this occurs even though the coherent activity of neurons that share the same receptive field is largely independent of the orientation of the stimulus [Figs. 1(b) and 1(c)].

(iv) The strength of the synchronization of the activity of neurons with different receptive fields is significantly enhanced by the use of a single, long bar that extends across several fields, rather than two discontinuous, short bars.

(v) The outputs of neurons with different receptive fields are not synchronized if the two stimuli move in opposite directions, even for neurons that respond vigorously to both directions of motion.

(vi) There are no substantial phase shifts in the temporal coherence for any of the experimental paradigms.

The existence of temporal synchronization over relatively large distances in the cortex suggests that, already in primary visual areas, the processing of information is a cooperative process that involves neurons with different receptive fields. The global aspects of this process challenge the classical notion that processing in the primary visual areas is essentially confined to segregated groups of neurons with discrete receptive fields (see also Ref. 9).

Oscillations in neuronal activity in the visual cortex and their potential role in computation have been the topic of much recent investigation.[10–22] Many of these works address the possible mechanisms that are responsible for the generation of cortical oscillations.[12–16,19–23] The discrimination of visual stimuli based on their relative orientation was studied by Sporns *et al.*[10,22] and by Schillen and Konig.[13,21] These investigations were based on computer simulations of models with relatively com-

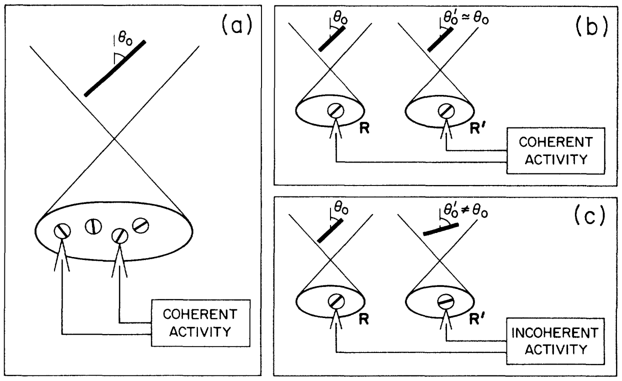

FIG. 1. Schematic summary of the experimental evidence on phase coherence between neurons in different regions of the cortex. The large ovals corresponds to the receptive field that is shared by different neurons (circles with stripes) whose individual orientation preference is indicated by the orientation of the stripe. The long bars correspond to stimuli with orientation θ_0. (a) The outputs of neurons that share the same receptive field are correlated, independent of their orientation preference. (b) The output of neurons in spatially separated receptive fields is correlated if the separate stimuli have the same relative orientation. (c) The output of neurons in spatially separated receptive fields is uncorrelated if the separate stimuli have the same relative orientation.

plex neuronal dynamics.

In this paper we present a model neural network that consists of neurons with oscillatory outputs. We study the temporal and spatial coherence of the oscillations and show that it can be strongly modulated by global features of an external stimulus. The capability of such a network to segment extended stimuli into distinct, coherent regimes according to the similarity of their local features is demonstrated.

We do not attempt to describe the mechanism that gives rise to the underlying oscillations. Rather, we consider a phenomenological description of interacting neuronal oscillators in the presence of noise in which the only dynamic variables are the phases of the oscillations. Such a description can, under certain circumstances, be systematically derived from the equations of motion of a system of weakly perturbed limit cycle oscillators.[24] We do not discuss the derivation of phase equations here. Phase equations of the form used in this study have been studied extensively as models of entrainment of populations of oscillators in physical and biological systems.[24,25] Models of phase oscillators have also recently been applied to the processing of visual stimuli.[11,17,18]

It is attractive to model the oscillatory responses in the visual cortex in terms of a phenomenological model of interacting phase oscillators with noise for a variety of reasons. First, it allows one to focus on the synchronization of the neuronal oscillations and the modulation of this synchrony. Second, the interactions that are required to synchronize the phases of two oscillators are much weaker than those required to modify their amplitudes. Our description thus implicitly assumes that the interactions that mediate and modulate the temporal synchronization between neuronal oscillators are substantially weaker than the intrinsic and extrinsic neuronal inputs that determine the average firing rate, or amplitude, of the neuronal response. This suggests that our model may act as a framework to reconcile the observed, long-range temporal synchronization with the localized, retinotopic organization of neuronal activity. Finally, the analysis of the network is greatly simplified by reducing the dynamical degrees of freedom of each neuron to a single phase.

We present an analytical and numerical study of the properties of our model. The theoretical analysis is greatly facilitated by our assumption that the interactions between the neurons are symmetric. This assumption allows us to describe the equilibrium properties of the network by statistical mechanics, similar to the description of interacting X-Y magnets. The analysis of the model is further facilitated by the presence of two scales of neuronal connectivity. Extensive connectivity within local clusters of neurons makes it possible to describe the short-range properties of the network by a mean-field theory. Long-range coherence is computed in terms of the interactions between the average phases for each of a small number of locally coherent clusters.

In Sec. II we define the phase equations and the pattern of connectivity. In Sec. III we analyze the feature specificity and discrimination of the model. In Sec. IV we present the mean-field analysis of the model and the main results of this analysis. In Sec. V we analyze the steady-state behavior of the system in terms of several examples of extended, orientation coded stimuli. In Sec. VI we study the effect of synaptic time delays. An extension of the model to include stimuli that are coded for direction as well as orientation is discussed in Sec. VII and an extension to account for possible modulation of the frequency of the oscillations by external stimuli is analyzed in Sec. VIII. Finally, we discuss some of the underlying assumptions of our model and the biological issues raised by them in Sec. IX.

Preliminary accounts of this work have been given.[26,27] Here we present a detailed analysis of the model. Furthermore, we incorporate a number of extensions that enhance the computational capabilities of the network.

II. MODEL

A. Stimuli

Our model describes the dynamic behavior of oscillatory neurons that respond to short bars in the visual field. Each neuron is sensitive to bars that are present within a receptive field located at $\mathbf{r}$. The size of the receptive field is small compared to that of the entire visual field. We initially focus on the behavior of neurons that respond only to the orientation of a bar, denoted by $\theta_0(\mathbf{r})$, where $0 \le \theta_0(\mathbf{r}) \le \pi$. Neurons that respond to this stimulus have an *average* rate of firing $\Gamma(\mathbf{r})$ that is described by

$$\Gamma(\mathbf{r}) = \Gamma(\theta_0(\mathbf{r}) - \theta(\mathbf{r})) , \tag{2.1}$$

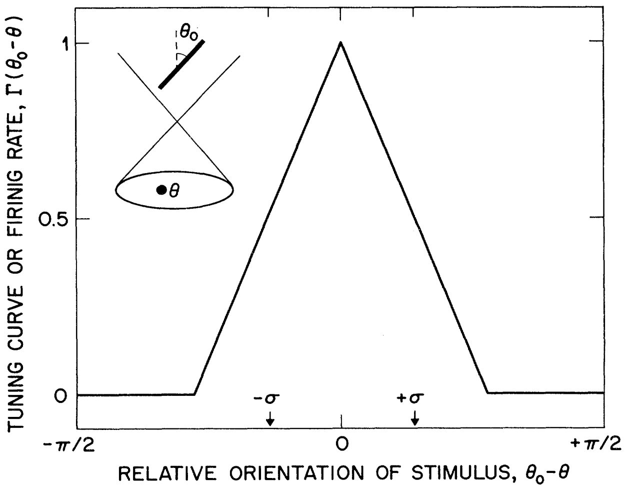

FIG. 2. Example of a tuning curve assumed for each of the neurons. The curve is the average firing rate of the neuron in response to a moving bar with orientation θ_0. The neuron has orientation preference θ. This particular curve has a triangular shape, given by $\Gamma(\theta_0-\theta)=(1-|\theta_0-\theta|/2\sigma)$ for $(\theta_0-\theta)<2\sigma$ and zero otherwise, where the half width at half maximum is $\sigma=0.44$ rad (25°).

where $\theta(\mathbf{r})$ is the orientation preferred by the neuron. We assume that there is a uniform distribution of preferred orientations among neurons that share the same receptive field. The dependence of the firing rate on the relative orientation of the stimulus, typically called the "tuning curve" of the neuron, is illustrated by the example in Fig. 2 (e.g., Ref. 28). Neurons that encode both the orientation and the direction of motion of moving bars will be considered later.

B. Phase variables

We describe the state of the neuron at time t by the instantaneous rate of firing $P(\mathbf{r},t)$. It is constructed by averaging the activity of the neuron over short periods of time, i.e., a few milliseconds, and is assumed to have the form

$$P(\mathbf{r},t)=\Gamma(\mathbf{r})[1+\lambda\cos\Phi(\mathbf{r},t)] \; . \tag{2.2}$$

The phases $\Phi(\mathbf{r},t)$ parametrize the time dependence of the firing pattern of the neurons. The coefficient λ corresponds to the relative contribution of the temporally modulated neuronal activity.

The observed neural responses exhibit bursts of spikes.[5] The time between each burst is close to periodic, while the time between individual spikes in a burst is highly irregular. We therefore identify the phase variables with the periodicity of the bursts, i.e., the coarse-grained firing rates, and not with the timing of individual spikes. The phases vary on the time scale of the average period of the oscillations, which is considerably longer than the shortest intervals between adjacent spikes.

C. Phase equations

The phase variables that govern the temporal aspects of the neuronal activity are assumed to obey equations for a system of coupled phase oscillators with noise, i.e.,

$$\dot{\Phi}(\mathbf{r},t)=\omega+\eta(\mathbf{r},t) - \sum_{\mathbf{r}'\,(\neq\mathbf{r})} J(\mathbf{r},\mathbf{r}')\sin[\Phi(\mathbf{r},t)-\Phi(\mathbf{r}',t)] \; , \tag{2.3}$$

where ω is the frequency of the neuronal oscillations and the term $\eta(\mathbf{r},t)$ represents fluctuations in the instantaneous frequency of a cell. It is taken to be white noise with variance $\langle\eta(\mathbf{r},t)\eta(\mathbf{r}',t')\rangle \propto \delta(t-t')$. The spatial correlations of $\eta(\mathbf{r},t)$ will be specified later. The connection strength $J(\mathbf{r},\mathbf{r}')$ mediates the interaction between the phases of the neurons at locations $\mathbf{r}$ and $\mathbf{r}'$. Finally, the sum over $\mathbf{r}'$ includes all neurons in the network.

D. Architecture of the connections

The interactions between the neuronal phases are assumed to encode information about the position and orientation of the stimulus. We postulate that they depend on the level of activity of the pre- and post-synaptic cell in a Hebb-like manner, i.e.,

$$J(\mathbf{r},\mathbf{r}')=V(\mathbf{r})W(\mathbf{r},\mathbf{r}')V(\mathbf{r}') \; , \tag{2.4}$$

where $V(\mathbf{r})$ is a function of $\Gamma(\mathbf{r})$, the average firing rate of the neuron [(2.1)]. This form allows the presence of an external stimulus to modulate interactions between neuronal phases. A particularly simple choice is

$$V(\mathbf{r})=\Gamma(\mathbf{r}) \; , \tag{2.5}$$

as assumed in our previous work.[26,27] However, as will be evident later, computational and sensitivity issues may require the use of a nonlinear relation. The term $W(\mathbf{r},\mathbf{r}')$ specifies the architecture of the connections and is independent of the external stimulus.

We assume an architecture for the network in which neurons are grouped into clusters, analogous to hypercolumns in the primary visual cortex (e.g., Refs. 29 and 30). The neurons in each cluster respond to a stimulus in a common receptive field. They are labeled by the spatial coordinates of the cluster, denoted $\mathbf{R}$, and their preferred orientation θ, which is assumed to be uniformly distributed within each cluster (Fig. 3).

Each neuron interacts with cells in the same cluster via short-range connections $W_{\mathbf{RR}}(\theta,\theta')$, taken as

$$W_{\mathbf{RR}}(\theta,\theta')=\frac{W_S}{N}F_S(\theta-\theta') \; , \tag{2.6}$$

where N is the total number of neurons in the cluster. Neurons in different clusters interact via long-range connections $W_{\mathbf{RR}'}(\theta,\theta')$, taken as

$$W_{\mathbf{RR}'}(\theta,\theta')=\frac{W_L}{N}F_L(\theta-\theta'), \quad \mathbf{R}\neq\mathbf{R}' \; . \tag{2.7}$$

We have assumed for simplicity that $W_{\mathbf{RR}'}(\theta,\theta')$ does not depend on the spatial separation between the clusters. The function $F_S(\theta-\theta')$ determines the feature specificity

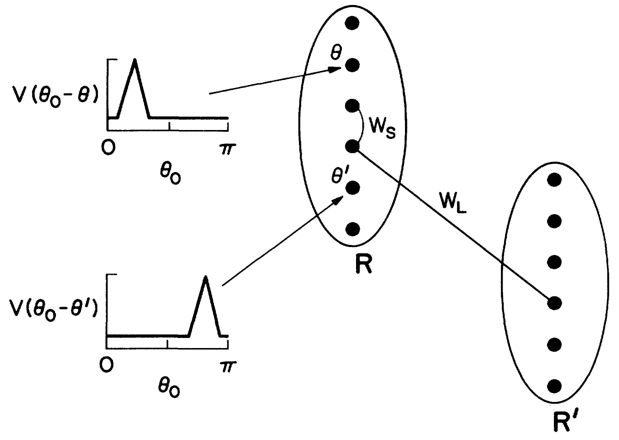

FIG. 3. Schematic of the neuronal architecture assumed in our model. Neurons that share a common receptive field are grouped into clusters. Each neuron interacts with cells in the same cluster via short-range connections with strength W_S/N and with cells in different clusters via long-range connections with strength W_L/N.

of the connections between neurons within a cluster, while the function $F_L(\theta-\theta')$ determines the feature specificity of the connections between neurons in different clusters. The relative strength of the long-range to short-range connections scales as

$$\frac{W_L}{W_S}\equiv\epsilon \ , \qquad (2.8)$$

where ϵ is assumed to be small ($\epsilon \ll 1$). This ensures that the coherence between neurons that share the same receptive field is largely independent of the *global* properties of the stimulus.

E. Spatial correlations of the noise

The extent of the synchronization between neurons within a cluster and between neurons in different cluster depends not only on the level of noise but also on the form of its spatial correlations. These noise characteristics will also determine the speed at which noninteracting neurons will be desynchronized. These correlations are, in general, expected to be related to the form of the neuronal architecture. In our architecture, it is natural to assume that the noise can be divided into two parts, i.e.,

$$\eta(\mathbf{r},t)=\zeta_{\mathbf{R}}(\theta,t)+\xi_{\mathbf{R}}(t) \ . \qquad (2.9)$$

The component $\zeta_{\mathbf{R}}(\theta,t)$ varies from neuron to neuron within the same cluster. It has variance

$$\langle \zeta_R(\theta,t)\zeta_{\mathbf{R}'}(\theta',t')\rangle = 2T_S\delta_{\mathbf{R}\mathbf{R}'}\delta_{\theta\theta'}\delta(t-t') \qquad (2.10)$$

and controls the coherence within a cluster. The component $\zeta_{\mathbf{R}}(\theta,t)$ is uniform for all neurons within a cluster, but varies between different clusters. It has variance

$$\langle \xi_{\mathbf{R}}(t)\xi_{\mathbf{R}'}(t')\rangle = 2T_L\delta_{\mathbf{R}\mathbf{R}'}\delta(t-t') \qquad (2.11)$$

and controls the coherence between different clusters. The relative strength of the two components of the noise are taken to be

$$\frac{T_L}{T_S}\sim\epsilon \ , \qquad (2.12)$$

so that both W_S/T_S and W_L/T_L are of the same order.

III. FEATURE SPECIFICITY AND DISCRIMINATION

A. Feature specificity of the connections

Our main focus is to study the synchronization between different clusters in response to global aspects of an extended stimulus. This synchronization is fairly insensitive to the detailed form of the fixed connections between neurons within the same cluster $F_S(\theta-\theta')$, but will depend strongly on the form of the orientation-specific long-range connections $F_L(\theta-\theta')$ between pairs of neurons belonging to different clusters. The relationship between $F_L(\theta-\theta')$ and the phase coherence between the clusters can be expressed in terms of the *effective* interaction, denoted $J_{\mathbf{R}\mathbf{R}'}$ between the *average* phases of the two clusters. A simplified form for $J_{\mathbf{R}\mathbf{R}'}$ is obtained by averaging the long-range interactions between all pairs of neurons belonging to the two clusters [(2.4), (2.6), and (2.7)]. This results in

$$J_{\mathbf{R}\mathbf{R}'}\simeq W_L\frac{N}{N_0}\frac{1}{\pi^2}\int_0^{\pi}\int_0^{\pi}d\theta\, d\theta' V_{\mathbf{R}}(\theta)F_L(\theta-\theta')V_{\mathbf{R}'}(\theta') \ , \qquad (3.1)$$

where

$$V_{\mathbf{R}}(\theta)\equiv V(\theta_0(R)-\theta(R)) \qquad (3.2)$$

and N_0 is the total number of neurons in the cluster for which the value of $V_{\mathbf{R}}(\theta)$ is not zero. Equation (3.1) is valid only in the limit that each cluster is fully synchronized, i.e., $W_S \gg T_S$. A more general form for the effective interaction, which is appropriate for $W_S\sim T_S$, is given in Sec. IV [(4.30)].

The ability of the network to discriminate between stimuli of different orientations is given by the dependence of $J_{\mathbf{R}\mathbf{R}'}$ on the orientation of the stimulus to the Rth cluster relative to that for the $\mathbf{R}'$th cluster. We define this difference as $\Delta\theta_0$, where

$$\Delta\theta_0\equiv\theta_0(\mathbf{R})-\theta_0'(\mathbf{R}') \ . \qquad (3.3)$$

The relation between $J_{\mathbf{R}\mathbf{R}'}$ and $\Delta\theta_0$ is readily seen by rewriting (3.1) as

$$J_{\mathbf{R}\mathbf{R}'}(\Delta\theta_0) \simeq W_L\frac{N}{N_0}\frac{1}{\pi^2}\int_0^{\pi}\int_0^{\pi}d\theta\, d\theta' V(\theta)F_L(\theta-\theta'+\Delta\theta_0)V(\theta') \ , \qquad (3.4)$$

where we have made use of (3.2) and the periodicity of $V_R(\theta)$. The form of $V_R(\theta)$ and $F_L(\theta-\theta')$ must be specified in order to evaluate the dependence of $J_{RR'}$ on $\Delta\theta_0$ [(3.4)]. Some general aspects of this dependence are presented below, followed by two specific examples.

B. Discrimination of features

We consider a form for the neuronal activity $V(\theta_0-\theta)$ that is essentially zero beyond an angle σ, i.e., $V(\theta_0-\theta)\simeq 0$ for $|\theta_0-\theta|>\sigma$. Similarly, we let $F_L(\theta-\theta')\simeq 0$ for $|\theta-\theta'|>\gamma$. Then

$$J_{RR'}(\Delta\theta_0)\simeq 0 \quad \text{for } |\Delta\theta_0|>2\sigma+\gamma \ . \tag{3.5}$$

The behavior of $J_{RR'}$ at small values of $\Delta\theta_0$ can be estimated by expanding (3.4) in powers of $\Delta\theta_0$. This yields

$$J_{RR'}(\Delta\theta_0)\simeq J_{RR'}(0)-A(\Delta\theta_0)^2, \quad \Delta\theta_0\simeq 0 \tag{3.6}$$

where

$$A=\frac{W_L}{2}\frac{N}{N_0}\frac{1}{\pi^2}\int_0^{\pi}\int_0^{\pi}d\theta\,d\theta'\frac{\partial V(\theta)}{\partial\theta}F_L(\theta-\theta')\frac{\partial V(\theta')}{\partial\theta'} \tag{3.7}$$

and we have assumed that $V(\theta)$ and $F_L(\theta-\theta')$ are even functions of their argument. A singularity occurs when $F_L(\theta-\theta')=\pi\delta(\theta-\theta')$ and $V(\theta)$ drops *discontinuously* at some angle θ_C. For this case, $J_{RR'}$ decreases linearly with the absolute value of $\Delta\theta_0$, i.e.,

$$J_{RR'}(\Delta\theta_0)\simeq J_{RR'}(0)-A|\Delta\theta_0|, \quad \Delta\theta_0\simeq 0 \tag{3.8}$$

where

$$A=\frac{W_L}{\pi}\frac{N}{N_0}(V_C)^2 \tag{3.9}$$

and V_C is the value of the discontinuity of V at θ_C. This result shows that, at least for small differences in orientation, a discontinuous drop in the activity $V(\theta_0-\theta)$ can substantially sharpen the sensitivity of the network to discriminate between stimuli.

C. Sharp discrimination with inhibitory connections

The tentative experimental results[4,6] and computational considerations suggest that $J_{RR'}$ is a rapidly decreasing function of $\Delta\theta_0$. It is not trivial to achieve this decrease in light of the above results [(3.5)] and the observation that the average extent of the tuning curves in the primary visual cortex is rather large, 0.9 rad (50°) or more.[28] One way to achieve a sharp dependence of $J_{RR'}$ on $\Delta\theta_0$ is to assume that $F_L(\theta-\theta')$ has an excitatory center and inhibitory surround. However, the inclusion of inhibitory components to $F_L(\theta-\theta')$ must be done with care so that $J_{RR'}$ does not assume negative values. Such values can lead to nonzero phase shifts among the oscillatory neurons. An example of an inhibitory scheme is [Fig. 4(a)]

$$F_L(\theta-\theta')=\left[1-\kappa^2\frac{\partial^2}{\partial(\theta-\theta')^2}\right]^2 e^{-(\theta-\theta')^2/2\rho^2}\ , \tag{3.10}$$

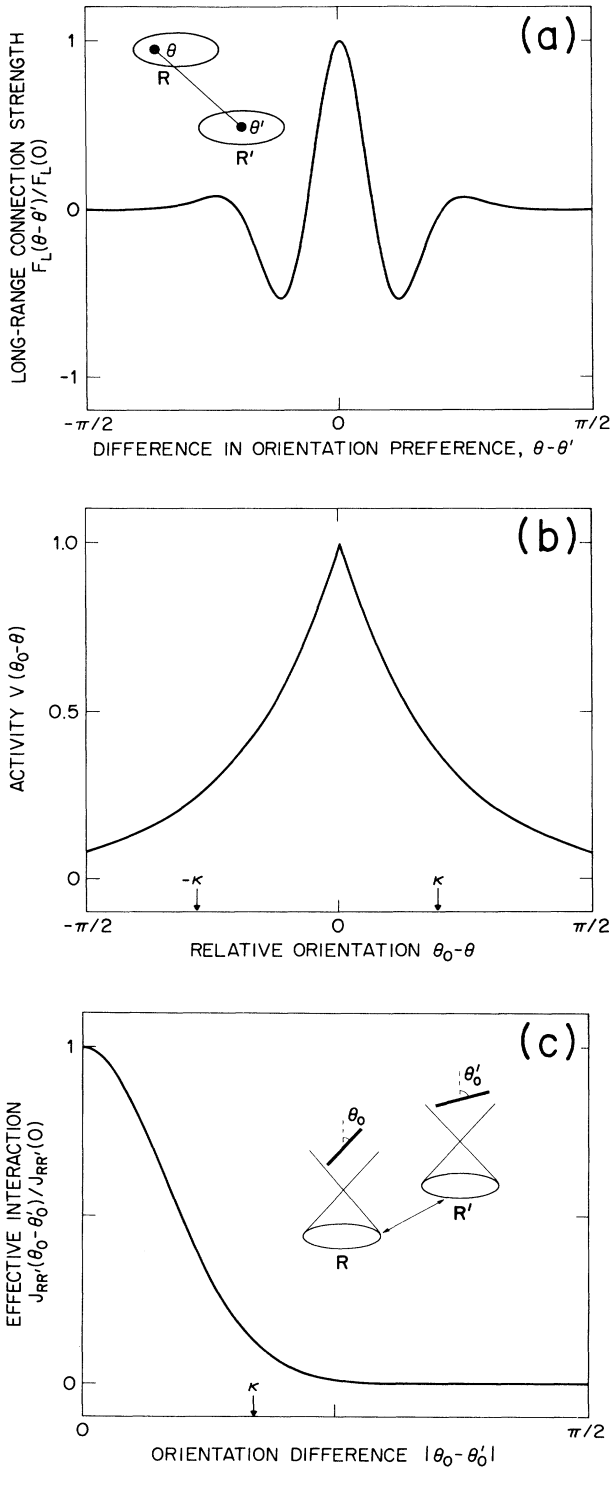

FIG. 4. The interaction between two spatially separated clusters that involves excitatory and inhibitory connections. (a) A form for the long-range connectivity between neurons in different clusters, with orientation preferences θ and θ', respectively [(3.10) and (A4)]. (b) The contribution of the activity of each neuron to the interaction between neuronal phases [(3.11)]. (c) The effective interaction between a pair of clusters for the connectivity in (a) [(3.12)].

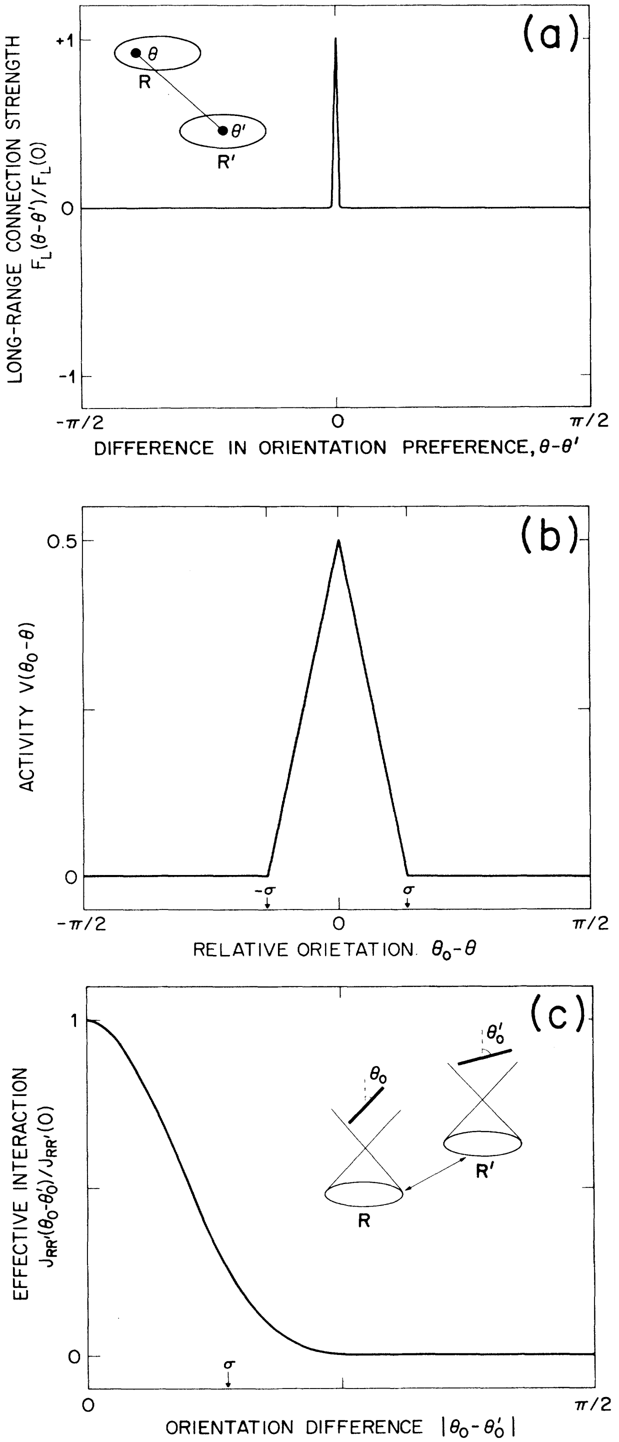

FIG. 5. The interaction between two spatially separated clusters that involves purely excitatory connections. (a) A form for the long-range connectivity between neurons in different clusters, with orientation preferences θ and θ', in which only neurons with similar orientation preferences form excitatory connections [(3.13)]. (b) The contribution of each neurons activity to the interaction between neuronal phases [(3.14)]. The curve is a thresholded version of the tuning curve shown in Fig. 2 [(3.16)]. (c) The effective interaction between a pair of clusters for the connectivity in (a) [(3.15)].

with $V_{\mathbf{R}}(\theta_0-\theta)$ of the form [Fig. 4(b)]

$$V_{\mathbf{R}}(\theta)=e^{-|\theta_0(\mathbf{R})-\theta(\mathbf{R})|/\kappa}\ , \tag{3.11}$$

where κ is the width of the activity curve. This choice yields [Fig. 4(c)]

$$J_{\mathbf{RR}'}\propto e^{-(\Delta\theta_0)^2/2\rho^2}\ , \tag{3.12}$$

where ρ is an independent parameter that determines the width of $J_{\mathbf{RR}'}$. This width can be considerably less than the width of the tuning curve. Details are given in Appendix A.

D. Discrimination with purely excitatory connections

Numerical simulations of the model using the above inhibitory scheme [(3.10) and (3.11)] have shown that it is not robust. Small distortions in the shape of $F_L(\theta-\theta')$ relative to that given by (3.7) disturb the delicate balance between excitation and inhibition. This tends to cause $J_{\mathbf{RR}'}$ to be negative for large values of $\Delta\theta_0$ and, as stated above, leads to phase locking of neurons with a phase shift of π. An alternative, robust choice for $F_L(\theta-\theta')$ is to include only excitatory components whose strength is a sharp function of the difference in angles $\theta-\theta'$ [Fig. 5(a)], i.e.,

$$F_L(\theta-\theta')=\pi\delta(\theta-\theta')=N\delta_{\theta,\theta'}\ . \tag{3.13}$$

The width of $J_{\mathbf{RR}'}$ is given by the width of $V(\theta_0-\theta)$ for this choice of $F_L(\theta-\theta')$ [(3.5)]. For concreteness, we assume that the activity $V(\theta_0-\theta)$ has a tentlike shape [Fig. 5(b)], i.e.,

$$V(\theta_0-\theta)=\begin{cases}\frac{1}{2}\left[1-\dfrac{|\theta_0-\theta|}{\sigma}\right], & |\theta_0-\theta|<\sigma\\ 0 \ \text{otherwise}\ . & \end{cases} \tag{3.14}$$

This hypothesis leads to

$$J_{\mathbf{RR}'}=\frac{W_L}{48\pi}\frac{2\sigma}{\pi}\frac{N}{N_0}\times\begin{cases}4-6x^2+3x^3 & \text{if } 0<x<1\\ (2-x)^3 & \text{if } 1<x<2\\ 0 \ \text{otherwise}\ , & \end{cases} \tag{3.15}$$

where $x=|\Delta\Theta_0|/\sigma$. The width σ must be substantially smaller than the width of the tuning curve (Fig. 2) in order to obtain sharp discrimination. To achieve this, we assume that the activity $V(\theta_0-\theta)$ is a strongly nonlinear function of the tuning curve $\Gamma(\theta_0-\theta)$. For $\Gamma(\theta_0-\theta)$ of the form shown in Fig. 2, (3.14) can be written as

$$V(\theta_0-\theta)=[\Gamma(\theta_0-\theta)-\Gamma_0]\Theta(\Gamma(\theta_0-\theta)-\Gamma_0)\ , \tag{3.16}$$

where the Heaviside function $\Theta(x)$ is 1 if $x>0$ and zero otherwise, and Γ_0 is a threshold parameter. The threshold is chosen to be $\Gamma_0=\frac{1}{2}$ in (3.14).

IV. ANALYSIS OF THE MODEL

A. Correlation functions

Before presenting our analysis of the model, we discuss the quantities that we wish to calculate. Coherent output in a population of neurons is deduced in experiments from the autocorrelogram of the output of each neuron and crosscorrelograms of the output of pairs of neurons.[31,32] The correlograms can be expressed in terms of the correlation functions of the underlying phase variables in the model. We define

$$\Phi_{\mathbf{R}}(\theta,t)=\omega t+\phi_{\mathbf{R}}(\theta,t)\ , \tag{4.1}$$

where ϕ represents the noisy component of the total phase Φ for a neuron in the **R**th cluster with orientation preference θ. The autocorrelogram is

$$\begin{aligned}&\langle P_{\mathbf{R}}(\theta,t)P_{\mathbf{R}}(\theta,t+\tau)\rangle\\&\qquad=\Gamma_{\mathbf{R}}^{2}(\theta)[1+(\lambda^2/2)C_{\mathbf{R}}(\theta,\tau)\cos(\omega\tau)]\ ,\end{aligned} \tag{4.2}$$

where $\langle\ \rangle$ denotes averaging over time and the autocorrelation function

$$C_{\mathbf{R}}(\theta,\tau)\equiv\langle\cos[\phi_{\mathbf{R}}(\theta,t)-\phi_{\mathbf{R}}(\theta,t+\tau)]\rangle \tag{4.3}$$

measures the temporal fluctuations in the phase. Note that the correlation functions are expected to depend only on the absolute value of the time τ and thus $\langle\sin[\phi_{\mathbf{R}}(\theta,t)-\phi_{\mathbf{R}}(\theta,t+\tau)]\rangle=0$. Furthermore, we have assumed that the averaging time is sufficiently long so that $\langle\cos(2\omega t)\rangle$ and $\langle\cos(\omega t)\rangle$ average to zero.

The crosscorrelogram of the activity of a neuron in the **R**th cluster with orientation preference θ with one in the **R**'th cluster with orientation preference θ' is

$$\begin{aligned}&\langle P_{\mathbf{R}}(\theta,t)P_{\mathbf{R}'}(\theta',t+\tau)\rangle\\&\quad=\Gamma_{\mathbf{R}}(\theta)\Gamma_{\mathbf{R}'}(\theta')\{1+(\lambda^2/2)C_{\mathbf{RR}'}(\theta,\theta',\tau)\\&\qquad\qquad\times\cos[\omega\tau+\chi_{\mathbf{RR}'}(\theta,\theta',\tau)]\}\ ,\end{aligned} \tag{4.4}$$

where the cross-correlation function $C_{\mathbf{RR}'}(\theta,\theta',\tau)$ measures the amplitude of the phase coherence and $\chi_{\mathbf{RR}'}(\theta,\theta',\tau)$ represents the average phase shift. These functions are given by $C_{\mathbf{RR}'}(\theta,\theta',\tau)=(a^2+b^2)^{1/2}$ and $\chi_{\mathbf{RR}'}(\theta,\theta',\tau)=\tan^{-1}(a/b)$ with $a\equiv\langle\sin[\phi_{\mathbf{R}}(\theta,t)-\phi_{\mathbf{R}'}(\theta',t+\tau)]\rangle$ and $b\equiv\langle\cos[\phi_{\mathbf{R}}(\theta,t)-\phi_{\mathbf{R}'}(\theta',t+\tau)]\rangle$. In all cases considered in this work, $a=0$ and thus

$$C_{\mathbf{RR}'}(\theta,\theta',\tau)=\langle\cos[\phi_{\mathbf{R}}(\theta,t)-\phi_{\mathbf{R}'}(\theta',t+\tau)]\rangle \tag{4.5}$$

and $\chi_{\mathbf{RR}'}(\theta,\theta',\tau)=0$.

B. Separation of scales

The equations for the phase of each neuron that incorporate the assumptions about the form of the connectivity [(2.3), (2.4), (2.6), and (2.7)] are

$$\begin{aligned}\dot\phi_{R}(\theta,t)=\zeta_{\mathbf{R}}(\theta,t)-\frac{W_S}{N}\sum_{\theta'}V_{\mathbf{R}}(\theta)F_S(\theta-\theta')V_{\mathbf{R}}(\theta')\sin[\phi_R(\theta,t)-\phi_{R'}(\theta',t)]\\+\xi_{\mathbf{R}}(t)-\frac{W_L}{N}\sum_{\mathbf{R}'(\neq\mathbf{R})}\sum_{\theta'(\neq\theta)}V_{\mathbf{R}}(\theta)F_L(\theta-\theta')V_{\mathbf{R}'}(\theta')\sin[\phi_{\mathbf{R}}(\theta,t)-\phi_{\mathbf{R}'}(\theta',t)]\ .\end{aligned} \tag{4.6}$$

The sum over θ' includes *all* neurons N in a cluster. The sum over **R**' includes *only* clusters that are activated by the stimulus. These equations can be written in the from

$$\dot\phi_{\mathbf{R}}(\theta,t)=\zeta_{\mathbf{R}}(\theta,t)+\xi_{\mathbf{R}}(t)-\frac{\partial E}{\partial\phi_{\mathbf{R}}}\ , \tag{4.7}$$

where the energy function E is

$$\begin{aligned}E[\phi]=-\frac{W_S}{2N}\sum_{\mathbf{R}}\sum_{\theta'(\neq\theta)}V_{\mathbf{R}}(\theta)F_S(\theta-\theta')V_{\mathbf{R}}(\theta')\cos[\phi_{\mathbf{R}}(\theta)-\phi_{\mathbf{R}}(\theta')]\\-\frac{W_L}{2N}\sum_{\mathbf{R}}\sum_{\mathbf{R}'(\neq\mathbf{R})}\sum_{\theta}\sum_{\theta'}V_{\mathbf{R}}(\theta)F_L(\theta-\theta')V_{\mathbf{R}'}(\theta')\cos[\phi_{\mathbf{R}}(\theta)-\phi_{\mathbf{R}'}(\theta')]\ .\end{aligned} \tag{4.8}$$

The energy function contains two terms. The intracluster term contributes an energy of order N, whereas the interaction between the clusters contributes a term of order ϵN. A similar separation holds for the dynamic equations [(4.7)], where the local noise $\zeta_{\mathbf{R}}(\theta,t)$ is responsible for the desynchronization of the intracluster degrees of freedom and the correlated noise $\zeta_{\mathbf{R}}(t)$ is responsible for desynchronizing the average phases of the clusters.

The intracluster degrees of freedom are

$$\delta\phi_{\mathbf{R}}(\theta)=\phi_{\mathbf{R}}(\theta)-\psi_{\mathbf{R}}\ , \tag{4.9}$$

where $\delta\phi_{\mathbf{R}}(\theta)$ measures the phase of each neuron relative to $\psi_{\mathbf{R}}$, the average phase of its cluster. Inspection of (4.6) shows that $|\partial\delta\phi_{\mathbf{R}}(\theta)/\partial t|$ has a value on the order of $\sim 1/T_S\sim 1/W_S$. In contrast, $|\partial\psi_{\mathbf{R}}/\partial t|$ is determined by long-range interactions, with overall strength $\sim\epsilon/W_S$, and by noise with magnitude of order $\sim\epsilon/T_S$. This implies that the coherence within a cluster can be studied by neglecting the long-range interactions. The coherence between clusters can then be determined by evaluating the slow fluctuations of the cluster phases $\psi_{\mathbf{R}}$.

C. Phase coherence within a single cluster

1. Mean-field equations

Neglecting terms of order ϵ, the dynamics of a single cluster are described by

$$\dot{\phi}_{\mathbf{R}}(\theta,t)=\zeta_{\mathbf{R}}(\theta,t) - \frac{W_S}{N}\sum_{\theta'\,(\neq\theta)} V_{\mathbf{R}}(\theta)F_S(\theta-\theta')V_{\mathbf{R}}(\theta') \times\sin[\phi_{\mathbf{R}}(\theta,t)-\phi_{\mathbf{R}'}(\theta',t)] \ . \tag{4.10}$$

These equations can be written as

$$\dot{\phi}_{\mathbf{R}}(\theta,t)=\zeta_{\mathbf{R}}(\theta,t)-\frac{\partial E_{\mathbf{R}}}{\partial\phi_{\mathbf{R}}} \ , \tag{4.11}$$

where the energy function of the Rth cluster is

$$E_{\mathbf{R}}=\text{const}-W_S\sum_{\theta} M_{\mathbf{R}}(\theta)V_{\mathbf{R}}(\theta)\cos[\phi_{\mathbf{R}}(\theta)-\psi_{\mathbf{R}}] \ . \tag{4.12}$$

The order parameters $M_{\mathbf{R}}(\theta)$ and $\psi_{\mathbf{R}}$ are defined by

$$M_{\mathbf{R}}(\theta)e^{i\psi_{\mathbf{R}}}\equiv\frac{1}{N}\sum_{\theta'} F_S(\theta-\theta')V_{\mathbf{R}}(\theta')e^{i\phi_{\mathbf{R}}(\theta')} \ . \tag{4.13}$$

In the limit of large N, the right-hand side of (4.13) can be replaced by its *thermal average*, i.e., by its average over ζ. Noting that the equilibrium distribution of $\phi_{\mathbf{R}}$ is given by a Boltzmann distribution with energy E [(4.12)], the order parameter $M_{\mathbf{R}}(\theta)$ is determined by the self-consistent condition

$$M_{\mathbf{R}}(\theta)=\frac{1}{\pi}\int_0^{\pi}d\theta' F_S(\theta-\theta')V_{\mathbf{R}}(\theta')m_{\mathbf{R}}(\theta') \ , \tag{4.14}$$

where

$$m_{\mathbf{R}}(\theta)\equiv\frac{\int_0^{\pi}d\phi\,\cos\phi\, e^{\beta_S W_S V_{\mathbf{R}}(\theta)M_{\mathbf{R}}(\theta)\cos\phi}}{\int_0^{\pi}d\phi\, e^{\beta_S W_S V_{\mathbf{R}}(\theta)M_{\mathbf{R}}(\theta)\cos\phi}} =\mathcal{H}(\beta_S W_S M_{\mathbf{R}}(\theta)V_{\mathbf{R}}(\theta)) \tag{4.15}$$

with $\beta_S\equiv 1/T_S$ and $\mathcal{H}(x)\equiv\mathcal{J}_1(x)/\mathcal{J}_0(x)$. The functions $\mathcal{J}_0(x)$ and $\mathcal{J}_1(x)$ are the modified Bessel function of zero and first order, respectively. In deriving the above equations we assumed that there are no phase shifts within a cluster, i.e., $\psi_{\mathbf{R}}$ is independent of θ. This may not be true if $F_S(\theta-\theta')$ has a strong inhibitory component.

In general, $M_{\mathbf{R}}(\theta)$ can be found by self-consistently solving (4.14) and (4.15) for a given $F_S(\theta-\theta')$. In the following analysis, we restrict ourselves to the simple choice of uniform excitatory connections within a cluster, i.e.,

$$F_S(\theta-\theta')=1 \ . \tag{4.16}$$

For this case, $M_{\mathbf{R}}(\theta)$ is independent of θ, i.e., $M_{\mathbf{R}}(\theta)=M_{\mathbf{R}}$, and thus

$$M_{\mathbf{R}}=\frac{1}{\pi}\int_0^{\pi}d\theta\, V_{\mathbf{R}}(\theta)m_{\mathbf{R}}(\theta) \ , \tag{4.17}$$

where

$$m_{\mathbf{R}}(\theta)=\mathcal{H}(\beta_S W_S M_{\mathbf{R}} V_{\mathbf{R}}(\theta)) \ . \tag{4.18}$$

The self-consistent equation for $M=M_{\mathbf{R}}$ is

$$M=\frac{1}{\pi}\int_0^{\pi}d\theta\, V_{\mathbf{R}}(\theta)\mathcal{H}[\beta_S W_S M V_{\mathbf{R}}(\theta)] \ . \tag{4.19}$$

Note that $m_{\mathbf{R}}(\theta)$ and $V_{\mathbf{R}}(\theta)$ depend on $\mathbf{R}$ only through angular differences, and thus the solutions of (4.19) are independent of $\mathbf{R}$.

2. *Emergence of phase coherence*

For high noise levels, i.e., T_S greater than a critical value T_C, the only solution of (4.19) is $M=0$, where the critical noise level T_C is

$$T_C=\frac{W_S}{2}\frac{1}{\pi}\int_0^{\pi}d\theta\, V_{\mathbf{R}}^2(\theta) \ . \tag{4.20}$$

We find $T_C=0.012W_S$ for $V_{\mathbf{R}}(\theta)$ of the form in Fig. 5(b) [(3.14)] with $\sigma=0.44$ rad (25°). This implies that all $m_{\mathbf{R}}(\theta)=0$ for noise levels $T_S>T_C$ and, consequently, that the noise desynchronizes the oscillations. Below T_C, the stable solution of (4.19) yields a value of M that is greater than zero. In the limit of low noise levels, i.e., $T_S\to 0$, the value of M approaches $\pi^{-1}\int_0^{\pi}d\theta\, V_{\mathbf{R}}(\theta)$. Hence, below T_C the value of $m_{\mathbf{R}}(\theta)$ for the active neurons is not zero. This signals the emergence of temporal phase coherence. The solution of (4.19) for M as a function of T_S/W_S, with $V_{\mathbf{R}}(\theta)$ given by (3.14), is shown in Fig. 6(a). The form of $m_{\mathbf{R}}(\theta)$ for several levels of noise is shown in Fig. 6(b). For values of T_S not far from T_C, the shape of $m_{\mathbf{R}}(\theta)$ has roughly the shape of $V_{\mathbf{R}}(\theta)$ [cf. Figs. 5(b) and 6(b)]. This can be seen analytically by examining (4.19) for small values of M. In contrast, for small values of T_S the value of $m_{\mathbf{R}}(\theta)$ saturates at a value close to 1 for all neurons that are significantly excited by the stimulus.

3. *Autocorrelation functions*

The value of $m_{\mathbf{R}}(\theta)$ measures the temporal coherence of the individual neurons. Specifically, the long-time limit of the autocorrelation function [(4.3)] is

$$\begin{aligned} C_{\mathbf{R}}(\theta) &\equiv \lim_{\tau\to\infty}\langle\cos[\phi_{\mathbf{R}}(\theta,t)-\phi_{\mathbf{R}}(\theta,t+\tau)]\rangle \\ &=\langle\cos[\delta\phi_{\mathbf{R}}(\theta,t)]\rangle\langle\cos[\delta\phi_{\mathbf{R}}(\theta,t+\tau)]\rangle \\ &=m_{\mathbf{R}}^2(\theta) \ . \end{aligned} \tag{4.21}$$

Note that $\phi_{\mathbf{R}}(\theta,t)$ fluctuates symmetrically about the average phase $\psi_{\mathbf{R}}$ [(4.9)] and thus $\langle\sin[\delta\phi_{\mathbf{R}}(\theta,t)]\rangle=0$.

To evaluate the time dependence of the autocorrelation function one has to analyze the dynamic equations [(4.6)]. Neglecting terms of order ϵ and using mean-field theory, the equations for $\delta\phi_{\mathbf{R}}(\theta,t)$ reduce to

$$\delta\dot{\phi}_{\mathbf{R}}(\theta,t)=\zeta_{\mathbf{R}}(\theta,t)-W_S M V_{\mathbf{R}}(\theta)\sin[\delta\phi_R(\theta,t)] \ . \tag{4.22}$$

When the level of noise is large, i.e., $T_S>T_C$, the autocorrelation functions decay to zero. Integrating (4.22) with respect to the Gaussian distribution for ζ and taking $M=0$ yields (Appendix B)

$$C_{\mathrm{R}}(\theta,\tau)=e^{-|\tau|T_S} . \tag{4.23}$$

When the level of noise is below T_C, the autocorrelation function decays from its initial value $C_{\mathrm{R}}(\theta,0)=1$ to its long-time limit $m_{\mathrm{R}}^2(\theta)$. This limiting value can be evaluated by numerical integration of (4.22). An approximate solution, valid for values of $m_{\mathrm{R}}(\theta)$ not too small, is (Appendix B)

$$C_{\mathrm{R}}(\theta,\tau)\simeq[1-m_{\mathrm{R}}^2(\theta)]e^{-|\tau|/\tau_S}+m_{\mathrm{R}}^2(\theta) , \tag{4.24}$$

where the decay constant τ_S is

$$\frac{1}{\tau_S}\simeq MW_S V_{\mathrm{R}}(\theta) . \tag{4.25}$$

The initial decay results in a peak in the autocorrelation function that is centered at $\tau=0$ and has a width of approximately $2\tau_S$.

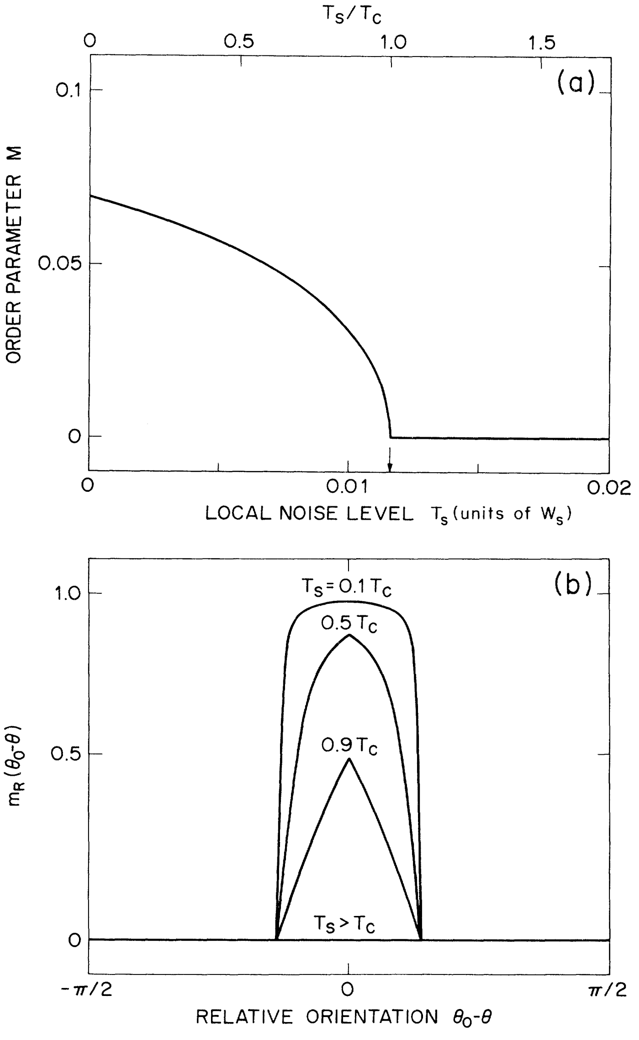

FIG. 6. Mean-field parameters for neurons in a single cluster. (a) The dependence of the order parameter M on the local noise level T_S. Equation (4.19) was solved numerically with the parameters $W_S=10$ and $\sigma=0.44$ [(3.14)], for which $T_C=0.12$. (b) The dependence of the long-time limit of the average phase $m_{\mathrm{R}}(\theta)=\langle\cos\delta\phi_{\mathrm{R}}(\theta)\rangle$ [(4.18)] on the orientation of the stimulus relative to the preferred orientation of the neuron. Equations (4.18) and (4.19) were solved numerically for different values of local noise level T_S, as indicated. Note that the intracluster correlation functions are given in terms of $m_{\mathrm{R}}(\theta)$ [(4.21) and (4.26)].

4. *Cross-correlations*

The intracluster cross-correlation functions factorize at all times τ since the direct interaction between a given pair of neurons is weak, i.e., of order $1/N$. Thus

$$\begin{aligned}C_{\mathrm{RR}}(\theta,\theta',\tau)&=\langle\cos[\phi_{\mathrm{R}}(\theta,t)-\phi_{\mathrm{R}}(\theta',t+\tau)]\rangle\\&=\langle\cos[\delta\phi_{\mathrm{R}}(\theta,t)]\rangle\langle\cos[\delta\phi_{\mathrm{R}}(\theta',t+\tau)]\rangle\\&=m_{\mathrm{R}}(\theta)m_{\mathrm{R}}(\theta') .\end{aligned} \tag{4.26}$$

Equations (4.21) and (4.26) imply that the cross-correlation is given by the geometric mean of the long-time limits of the autocorrelations, i.e.,

$$C_{\mathrm{RR}}(\theta,\theta',\tau)=[C_{\mathrm{R}}(\theta)C_{\mathrm{R}}(\theta')]^{1/2} . \tag{4.27}$$

Furthermore, there are no phase shifts associated with the cross-correlation, i.e., $\chi_{\mathrm{RR}}(\theta,\theta',\tau)=0$ [(4.4)] as the short-range connections are excitatory [(4.16)]. Thus all of the active neurons in a cluster will fire coherently as a result of the extensive short-range connectivity. Finally, according to (4.26), there is no peak centered near $\tau=0$ that is associated with the cross-correlation functions.

5. *Damping of the correlation functions by correlated noise*

Until now we have neglected all terms of order ϵ in our analysis of the intracluster equations. This includes the uniform, weak noise that is correlated within the cluster, i.e., $\xi_R(t)$ [(2.9)]. It is of interest to consider the effect of the cluster noise on the properties of a single stimulated cluster. The only change in the phase equations [(4.10)] is the addition of a term $\xi_{\mathrm{R}}(t)$. However, if one shifts all the phases of the neurons in the cluster by a global phase $\Psi_{\mathrm{R}}(t)$, whose time derivative is $\xi_{\mathrm{R}}(t)$, the equations of the shifted variables are identical to those of (4.10). This implies that the effect of a uniform cluster noise is to multiply the correlation functions found without this noise [(4.24) and (4.26)] by the autocorrelation $\langle\cos[\psi_{\mathrm{R}}(t)-\psi_{\mathrm{R}}(t+\tau)]\rangle=e^{-|\tau|T_L}$. Thus the noise $\xi_{\mathrm{R}}(t)$ induces a slow, exponential decay of the correlation function with a decay time of $1/T_L$. The long-time limit referred to above corresponds to time scales τ obeying $1/T_C\ll\tau\ll1/T_L$.

D. Numerical results for stimulation of a single cluster

We carried out numerical simulations of the phase equations [(4.6)] with a network consisting of one active cluster that contained 1000 phase oscillators. The orientation selectivity of the oscillators was uniformly distributed between $\theta=-\pi/2$ and $\pi/2$, with activity dependences as shown in Fig. 5(b). The short-range connection strengths W_S were uniform [(4.16)]. We performed simulations for local noise levels T_S both below and above T_C and for zero and nonzero levels of correlated noise T_L. The correlation functions $C_{\mathrm{R}}(\theta,\tau)$ and $C_{\mathrm{RR}}(\theta,\theta',\tau)$ were calculated from the time dependence of the phase variables [(4.21) and (4.26)] averaged over an interval of $1\times10^4/T_C$. The results of these simulations are compared with the numerical solution of the mean-field equation [(4.22) with M given by (4.19) for $T_S<T_C$ and (4.23) for $T_S>T_C$].

The time dependence of the autocorrelation function of a neuron that is optimally stimulated, i.e., $\theta=\theta_0$, is shown in Fig. 7. In all cases, the results obtained from the mean-field theory (solid lines) agree very well with those obtained from numerical simulations of the phase equations (solid circles). This implies that the finite-size corrections at $N=1000$ to the $N\rightarrow\infty$ behavior are rather small. We consider first the behavior of the autocorrelation function with $T_L=0$. This function shows a fast decay from its initial value of 1 to a long-time limit for noise levels $T_S<T_C$ (Fig. 7). The limiting value is consistent with the value of $C_{\mathrm{R}}(\theta_0)$ calculated [(4.18), (4.19), and (4.21)] for the parameters used in the simulation. For noise levels $T_S>T_C$, the autocorrelation decays rapidly to zero (Fig. 7). In the presence of correlated noise, i.e., $T_L\neq0$, the autocorrelation functions are observed to exhibit two time constants (Fig. 7). The initial decay to a nonzero value occurs with time constant τ_S [(4.25)], while the slow decay to zero occurs with a time constant close to $1/T_L$, as predicted (Sec. IV C).

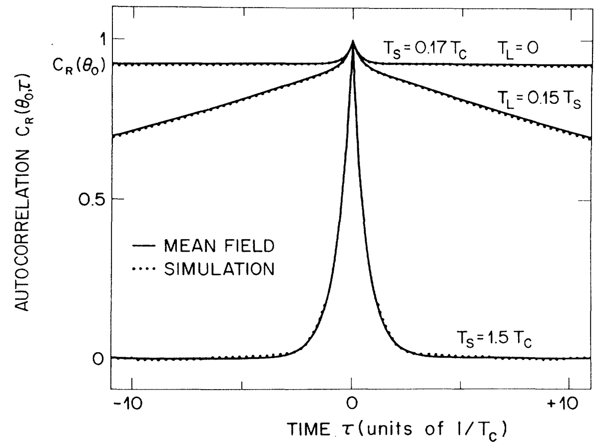

FIG. 7. The autocorrelation function $C_{\mathrm{R}}(\theta,\tau)$ of a neuron that is stimulated by a moving bar at the preferred orientation of the neuron, i.e., $\theta=\theta_0$. Results are shown for three levels of noise: (i) $T_S=0.020=0.17T_C$ and $T_L=0$, (ii) $T_S=0.020=0.17T_C$ and $T_L=0.0030=0.026T_C$, and (iii) $T_S=0.17=1.5T_C$ and $T_L=0$. The dotted line is the result found from simulation of the phase equations. Equation (4.4) was solved numerically for a single, active cluster with $N=1000$, $V(\theta-\theta_0)$ given by (3.14) with $\sigma=0.44$ rad, $F_S(\theta-\theta')=1$ [(4.16)], $W_S=10$, $F_L(\theta-\theta')=0$. Equations [(4.4)] was solved with a time step $\Delta t=1.0$ and the autocorrelation functions were calculated [(4.3)] by averaging over 130 000 time steps. The solid line is the result of the numerical solution of the mean-field equation [(4.22)]. In the presence of correlated noise, i.e., $T_L=0.15T_S$. The autocorrelation function calculated from (4.22) was multiplied by $\exp(-|\tau|T_L)$.

The time dependence of the autocorrelation and cross-correlation functions for a pair of neurons, with $\theta=\theta_0=0$ and $\theta'=0.8\sigma=0.35$ rad are shown in Fig. 8. We consider the case with $T_L=0$ to emphasize the difference in the time dependence between the cross-correlation function and autocorrelation functions. The observed reduction in the long-time value of the autocorrelation function of the suboptimally stimulated neuron $C_{\mathrm{R}}(\theta',\tau)$ is in accordance with the mean-field result [Fig. 6(b)]. The cross-correlation function $C_{\mathrm{R}}(\theta,\theta',\tau)$ is essentially constant in time. Its value is also in good agreement with that predicted from the mean-field theory [(4.27)].

Time scale of the oscillations

The above results illustrate how the time course of the correlation functions markedly depends on the level of noise relative to the critical level T_C [(4.20)]. This suggests that T_C should correspond to the noise level below which persistent oscillations can occur in the network. Thus, on one hand, the neurons should behave as overdamped oscillators for noise levels $T_S>T_C$. This condition is achieved for periods $2\pi/\omega>1/T_C$. On the other

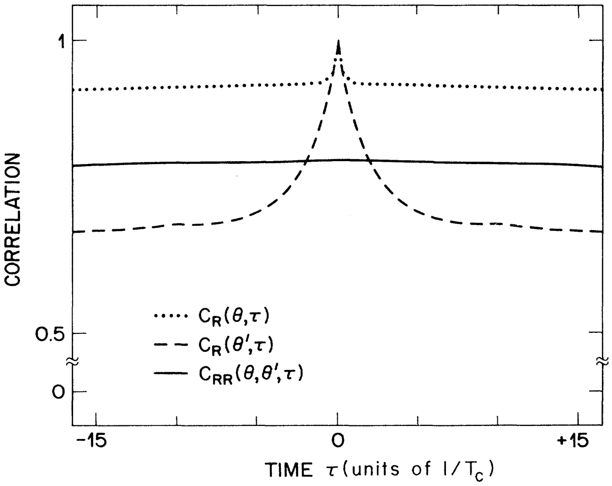

FIG. 8. The auto- and cross-correlation functions for two neurons in a single cluster that are stimulated by a moving bar. One of them is stimulated at its preferred orientation, i.e., $\theta-\theta_0=0$ and the other at the nonoptimal orientation $\theta-\theta_0=0.35$ rad (20°). The correlations [(4.3) and (4.5)] were found from numerical simulation of the phase equations [(4.6)] with $T_S=0.02=0.17T_C$ and $T_L=0$ and all other parameters as in Fig. 7.

hand, the neurons should exhibit persistent, coherent activity when the level is below T_C. This implies that the period of the oscillations should be smaller than the long-time decay of the correlation functions, given by $1/T_L$. Thus the period of the oscillations is conjectured to lie in the range $1/T_C \lesssim 2\pi/\omega \lesssim 1/T_L$. This point is illustrated by the correlograms [(4.2) and (4.4)] in Fig. 9, for which we chose $2\pi/\omega = 2/T_C \simeq 0.05/T_L$ [the parameters are otherwise the same as those used above (Fig. 9)]. Slowly decaying, coherent oscillations are observed only for the case of $T_S < T_C$.

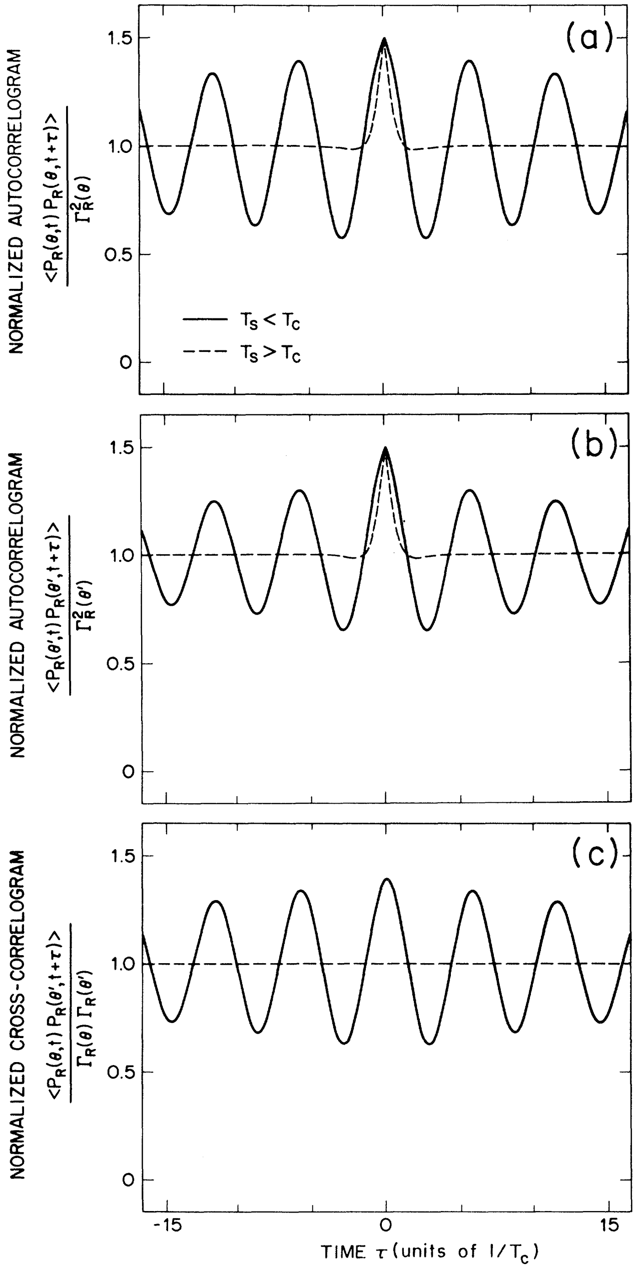

FIG. 9. The normalized auto- and cross correlograms, which includes the oscillatory part of the neuronal response, for neurons in a cluster that is stimulated by a moving bar. One neuron is stimulated at its preferred orientation, i.e., $\theta - \theta_0 = 0$ and the other at a nonoptimal orientation, i.e., $\theta - \theta_0 = 0.35$ rad (20°). The correlograms [(4.2) and (4.4)] were found from numerical simulation of the phase equations [(4.6)] with $T_S = 0.02$ and $T_L = 0.003$ and all other parameters as in Fig. 8. The period of the oscillations was chosen to lie between T_C ($T_C = 0.12$ for our parameters) and T_L.

E. Coherence between spatially separated clusters

1. *Effective interactions between clusters*

The intracluster energy does not determine the values of the mean cluster phases $\psi_{\mathbf{R}}$, since shifting all the phases of a given cluster does not affect its energy. The cluster phases are determined by the intercluster term of (4.8). An effective energy function for the cluster phases is derived by averaging the intercluster term over the local noise $\zeta_{\mathbf{R}}(\theta,t)$ or, equivalently, over the fast fluctuations of the intracluster degrees of freedom. This yields

$$E[\psi] \simeq -\frac{W_L}{2N} \sum_{\mathbf{R}} \sum_{\mathbf{R}'(\neq \mathbf{R})} \sum_{\theta} \sum_{\theta'} V_{\mathbf{R}}(\theta) F_L(\theta-\theta') V_{\mathbf{R}'}(\theta') \times \langle \cos[\delta\phi_{\mathbf{R}}(\theta) - \delta\phi_{\mathbf{R}'}(\theta') + \psi_{\mathbf{R}} - \psi_{\mathbf{R}'}] \rangle , \tag{4.28}$$

where $\langle \; \rangle$ refers to averaging over the $\delta\phi$. Using $\langle \cos[\delta\phi_{\mathbf{R}}(\theta) - \delta\phi_{\mathbf{R}'}(\theta')] \rangle = m_{\mathbf{R}}(\theta) m_{\mathbf{R}'}(\theta')$ and $\langle \sin[\delta\phi_{\mathbf{R}}(\theta) - \delta\phi_{\mathbf{R}'}(\theta')] \rangle = 0$, one obtains

$$E[\psi] = -\tfrac{1}{2} \sum_{\mathbf{R}} \sum_{\mathbf{R}'(\neq \mathbf{R})} J_{\mathbf{RR}'} \cos(\psi_{\mathbf{R}} - \psi_{\mathbf{R}'}) , \tag{4.29}$$

where the effective interaction between the cluster phases $J_{\mathbf{RR}'}$ is

$$J_{\mathbf{RR}'} = W_L \frac{N}{N_0} \frac{1}{\pi^2} \int_0^{\pi} \int_0^{\pi} d\theta \, d\theta' \, V_{\mathbf{R}}(\theta) m_{\mathbf{R}}(\theta) \times F_L(\theta - \theta') V_{\mathbf{R}'}(\theta') m_{\mathbf{R}'}(\theta') . \tag{4.30}$$

For the relevant case of $V_{\mathbf{R}}(\theta) = 0$ for $|\theta_0 - \theta| > 0$ [(3.14)], the number of active neurons is $N_0 = (2\sigma/\pi)N$. Finally, note again that $J_{\mathbf{RR}'}$ is a function only of the difference in the orientation of the stimuli $\Delta\theta_0 \equiv \theta_0(\mathbf{R}) - \theta_0'(\mathbf{R}')$.

The temporal fluctuations in the $\psi_{\mathbf{R}}$ are affected by the *cluster* noise $\xi_{\mathbf{R}}(t)$. Both the effective coupling between the cluster phases $J_{\mathbf{RR}'}$ and the effective dephasing noise are of the same order, i.e., the value of ϵ. As a consequence, the cluster phases vary on the time scale $\tau_L = 1/T_L \simeq 1/(\epsilon T_S)$ and the dynamics of $\psi_{\mathbf{R}}$ can be approximated by

$$\dot{\psi}_{\mathbf{R}}(t) = \xi_{\mathbf{R}}(t) - \sum_{\mathbf{R}'(\neq \mathbf{R})} J_{\mathbf{RR}'} \sin[\psi_{\mathbf{R}}(t) - \psi_{\mathbf{R}'}(t)] . \tag{4.31}$$

2. *Correlation functions*

The cross-correlation function between the output of neurons in different clusters can be expressed, using the above results, as

$$\begin{aligned}C_{RR'}(\theta,\theta',\tau)&=\langle\cos[\phi_R(\theta,t)-\phi_{R'}(\theta',t+\tau)]\rangle\\&=\langle\cos[\delta\phi_R(\theta,t)]\rangle\langle\cos[\delta\phi_{R'}(\theta',t+\tau)]\rangle\\&\quad\times\langle\cos[\psi_R(t)-\psi_{R'}(t+\tau)]\rangle\ . \qquad (4.32)\end{aligned}$$

Equations (4.21) and (4.32) imply that the correlation between different clusters has the form

$$\begin{aligned}C_{RR'}(\theta,\theta',\tau)&=m_R(\theta)m_{R'}(\theta')C_{RR'}(\tau)\\&=[C_R(\theta)C_{R'}(\theta')]^{1/2}C_{RR'}(\tau)\ , \qquad (4.33)\end{aligned}$$

where

$$C_{RR'}(\tau)\equiv\langle\cos[\psi_R(t)-\psi_{R'}(t+\tau)]\rangle \qquad (4.34)$$

measures the correlation of the mean phases of the two clusters.

As noted above, $C_{RR'}(\tau)$ depends appreciably on τ only for $\tau\gtrsim 1/T_L$. As long as one considers the coherence between clusters for time intervals that are short compared to $1/T_L$, the time dependence of $C_{RR'}$ can be neglected. In this limit, the coherence between clusters can be evaluated by the equilibrium *equal-time* correlation functions $C_{RR'}\equiv C_{RR'}(0)$ for a system described by the energy function $E[\psi]$ of (4.29).

We emphasize that our simple result for the dynamics of the collective degrees of freedom, i.e., the cluster phases ψ_R [(4.31)], are exact only in the limit $T_S \ll T_C$. In this limit the fluctuations in the intracluster degrees of freedom can be neglected. In the general case, (4.30) and (4.31) are probably only approximately valid and even the notion of a cluster phase requires a more precise definition. For instance, a naive definition of ψ_R in terms of a simple average of the individual phases may not coincide exactly with the phase that is defined through the equation for the order parameter M [(4.13)]. Our applications of the theoretical results in the examples below are all in the regime of $T_S \ll T_C$, where these differences are negligible.

V. EXAMPLES

The correlation function between a pair of clusters $C_{RR'}$ depends on the direct interaction between the two clusters as well as the indirect interaction via other active clusters. We consider below several examples of extended stimuli and demonstrate the dependence of the coherence $C_{RR'}$ [(4.33)] on global features of the stimulus. For each example, we use the long-range connectivity $F_L(\theta-\theta')=\pi\delta(\theta-\theta')$, a tentlike shape for $V_R\ (\theta)$ [(3.14)] with $\sigma=0.44$ rad (25°), and the associated form for $J_{RR'}$ [(3.16)].

A. Stimulation by two short bars

The simplest example of long-range coherence involves two clusters that are stimulated by separate, short bars whose length spans the individual receptive fields.

1. *Analytical results*

Denoting the relative phases of the two clusters by $\psi\equiv\psi_R-\psi_{R'}$, the relevant energy function reduces to

$$E[\psi]=-J_{RR'}\cos\psi\ . \qquad (5.1)$$

The resultant correlation function is

$$C_{RR'}=\frac{\int_0^\pi d\psi(\cos\psi)e^{\beta_L J_{RR'}\cos\psi}}{\int_0^\pi d\psi e^{\beta_L J_{RR'}\cos\psi}}=\mathcal{H}(\beta_L J_{RR'})\ , \qquad (5.2)$$

where

$$\beta_L\equiv\frac{1}{T_L}\simeq\frac{\beta_S}{\epsilon} \qquad (5.3)$$

and the form of $J_{RR'}$ is specified by (3.15). The dependence of the equal-time cross-correlation on the *relative* orientation of the bars, $\Delta\theta_0=\theta_0-\theta_0'$, is shown in Fig. 10.

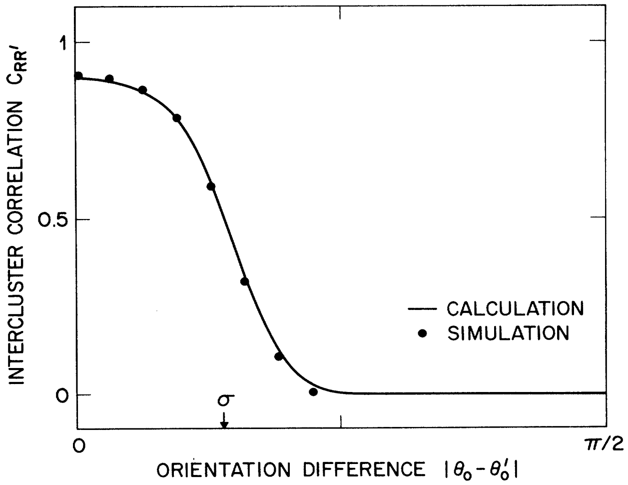

FIG. 10. The equal-time cross-correlation between the cluster phases ψ_R and $\psi_{R'}$ of two clusters stimulated by short bars. The difference in orientation between the bars is $\Delta\theta_0$. The solid line is the analytical result [(5.2) with $J_{RR'}$ of (3.15)]. The circles represent results derived from numerical simulation of the phase equations for a network with two active clusters for which the cluster phases were calculated according to (4.13). For this example, long-range excitatory connections existed only between neurons with similar orientation preferences [(3.13)], the activity of each neuron was described by the curve in Fig. 15(b), and the short-range connectivity was taken as uniform [(4.16)]. The other parameters were $W_S=10$, $W_L=0.2$, $T_S=0.02\simeq0.17T_C$, and $T_L=0.003\simeq0.026T_C$. For the numerical simulations, (4.6) was simulated for two clusters, each containing $N=1000$ neurons. The time step was $\Delta t=1.0$ and the autocorrelation functions were calculated [(4.34)] by averaging over 170 000 time steps.

2. *Numerical results*

We carried out numerical simulations of the phase equations for the case of two clusters, each simulated by a short bar. The parameters for these simulations were identical, when appropriate, to those for the numerical simulation for one cluster (Figs. 7–9). We calculated the global phase $\psi_{\mathbf{R}}(t)$ [(4.13)] for each cluster. The cross-correlation $C_{\mathbf{RR}'}(\tau)$ [(4.34)] was calculated from the time dependence of the global phases, averaged over an interval of $2\times10^4/T_C$, for three values of $\Delta\theta_0$ (Fig. 11). Note that the decay time of the cross-correlations is long, of order $1/T_L \simeq 40/T_C$ for the parameters used in the simulations. The fluctuations in the cross-correlations for $\Delta\theta_0 = 1.5\sigma$ reflect insufficient averaging time.

The equal-time cross-correlation determined from the simulations, i.e., $C_{\mathbf{RR}'}(0)$, is shown along with analytical results in Fig. 10. The agreement between the analytical results and the results of the numerical simulations is very good. The correlation is nearly $C_{\mathbf{RR}'} = 1$ for $\Delta\theta_0 = 0$ and decreases quadratically for small values of $\Delta\theta_0$, in accordance with (3.6). For large values of $\Delta\theta_0$ the cross-correlation decreases rapidly. It vanishes for $\Delta\theta_0 = 2\sigma$, in agreement with (3.15). However, already at $\Delta\theta_0 = \sigma$ the cross-correlation decreases by a factor of 2 compared with the value at $\Delta\theta = 0$.

B. Extended bar

As the length of the bar increases, the correlation between a pair of excited clusters is enhanced. To demonstrate this effect, we evaluated $C_{\mathbf{RR}'}$ for the case of a straight bar that spans K receptive fields and thus activates K clusters. The energy function can be written as

$$E[\psi] = -\frac{J_{\mathbf{RR}'}}{2}\sum_{\mathbf{R}}\sum_{\mathbf{R}'(\neq\mathbf{R})}\cos(\psi_{\mathbf{R}} - \psi_{\mathbf{R}'}) \ . \tag{5.4}$$

The calculation of $C_{\mathbf{RR}'}$ is presented in Appendix C. Qualitatively, the value of the correlation depends on the length K relative to the characteristic length K_C, where

$$K_C \equiv \tfrac{1}{2}\beta_L J_{\mathbf{RR}'} \ . \tag{5.5}$$

The correlation is small for $K/K_C \ll 1$ and is saturated at a value near 1 for $K/K_C \gg 1$. Examples of the dependence of $C_{\mathbf{RR}'}$ on K for two values of K_C are shown in Fig. 12. The enhancement of the coherence with increasing values of K is pronounced for $K_C < 1$ (Fig. 12). There is only modest enhancement in the correlation for the opposite case $K_C > 1$ since the correlation saturates even when two receptive fields are activated. The experimental evidence[6] for an enhanced correlation when the stimulus is a long bar suggests that $K_C \lesssim 1$.

C. Extended curved objects

The curvature of stimuli that span several receptive fields can be used to segment a stimulus into separate objects. We illustrate this by considering the coherence between clusters in the presence of K bars with orientations that vary in space. The bars were arranged in either a smooth, continuous manner, representing a single object [Fig. 13(a)], or in a discontinuous manner, representing two distinct objects [Fig. 13(b)]. The total angle spanned by the stimulus $\Delta\theta_0$ is the same for both arrangements.

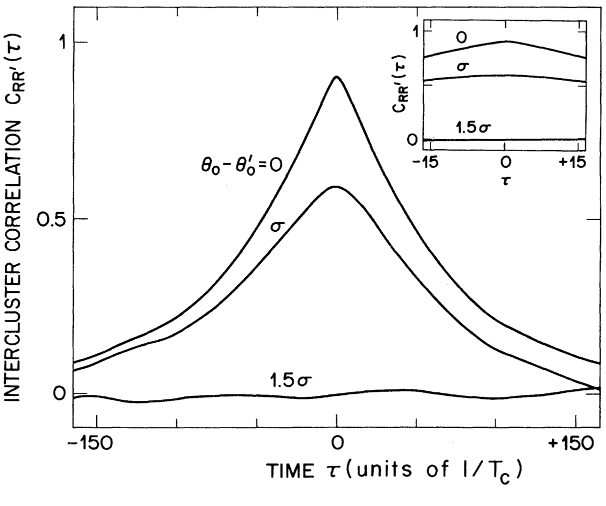

FIG. 11. The cross-correlation $C_{\mathbf{RR}'}(\tau)$ between the global phases $\Psi_{\mathbf{R}}$ of two clusters as a function of the difference in orientations of the respective stimuli $\Delta\theta_0$. These results were derived from numerical simulations of (4.6), using the parameters given in the legend to Fig. 10. The insert shows the time dependence near $\tau=0$ on an expanded scale for comparison with Fig. 8.

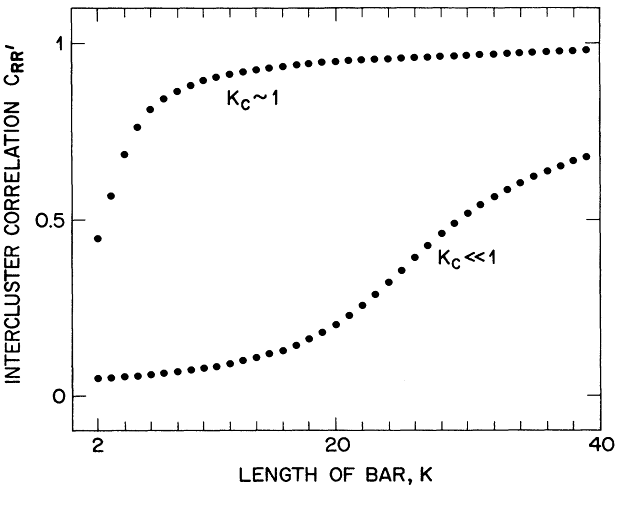

FIG. 12. The enhancement in the correlation between two spatially separated clusters that are stimulated by a single moving long bar, as opposed to two collinear short bars [(5.4)]. The length of the bar K is expressed as the number of receptive fields that it spans. The upper curve is for a characteristic length $K_C = 1$ and the lower curve is for $K_C = 0.1$ [(5.5)].

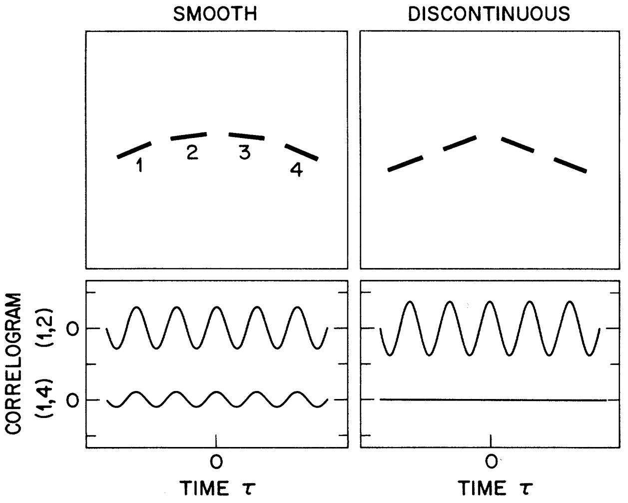

FIG. 13. Segmentation of four oriented bars that span several receptive fields. The bars are of equal length and spacing and are arranged to subtend the same total angle ($W_L/T \simeq 7$). (a) Bars arranged as a smoothly varying stimulus. (b) Bars arranged as discontinuous stimuli. (c) The pairwise correlations between adjacent clusters are equal [$C_{12}=C_{23}=C_{34}\approx 0.6$ with $\Delta\theta_0=0.26$ rad (15°)]. Neurons in all of the active clusters fire coherently and the end-to-end correlation is $C_{14}=(C_{12})^3\approx 0.2$. (d) The pairwise correlations between adjacent clusters are $C_{12}=C_{34}\approx 0.8$ [$\Delta\theta_0=0$] and $C_{23}\approx 0$ [$\Delta\theta^0=\pi/4$ rad (45°)]. The end-to-end correlation is $C_{14}\approx 0$.

We chose $\Delta\theta_0=\pi/4$ rad (45°) for the examples shown in Fig. 13.

1. Continuous stimulus

The interactions between proximal clusters will induce correlations among the neurons in all of the clusters. This represents a classification of the stimulus as a single object. To calculate the strength of the correlations between pairs of clusters, let us assume that the only significant interactions are those between nearest neighbors, i.e., $J_{\mathbf{RR}'}(\delta\theta_0)$, where $\delta\theta_0=\Delta\theta_0/(K-1)$. The system is then equivalent to a finite chain of phases that are coupled by a nearest-neighbor interaction with an energy function

$$E=-\tfrac{1}{2}J_{\mathbf{RR}'}(\delta\theta_0)\sum_{i=1}^{K-1}\cos(\psi_i-\psi_{i+1}) \;. \tag{5.6}$$

The resultant correlation function between the ith and the jth clusters C_{ij}, is

$$C_{ij}=[\mathcal{H}(\beta_L J_{\mathbf{RR}'}(\delta\theta_0))]^{|i-j|} \tag{5.7}$$

and is characteristic of the form of correlation functions found for one-dimensional systems. If $\beta_L J_{\mathbf{RR}'}(\delta\theta_0)$ is not too small, substantial correlations will exist even between neurons that are far apart [Fig. 13(a)].

2. Discontinuous stimulus

We assume that $J_{\mathbf{RR}'}(\Delta\theta_0)\sim 0$. The neurons in each group of $K/2$ clusters will fire coherently, but there is negligible coherence between the two groups. Thus the network forms two separate coherent regimes [Fig. 13(b)]. The regimes represent a segmentation of the stimulus into two distinct objects.

VI. TIME DELAYS AND PHASE SHIFTS

We have assumed so far that the interactions between phases are predominantly positive and have zero time delays. Thus the absence of phase shifts is expected. However, the local connections between cortical neurons are mediated by unmyelinated axons with slow propagation speeds, i.e., approximately 1 mm/ms.[30] It is thus important to investigate the effect of time delays on the synchronization of oscillations and, in particular, on the phase shifts between the output of different neurons.

The propagation delay time for distances of the order of 1 mm is approximately 1 ms, which is much smaller than the period of the oscillations $2\pi/\omega\sim 25$ ms. Thus the delays are not expected to affect the synchronization within a cluster. On the other hand, the axonal delays between synchronized neurons that are separated by 7–10 mm cannot be ignored. To study the effect of the delays in the long-range connections, we consider the synchronization of two active clusters described by phase equations with delayed interactions, i.e.,

$$\begin{aligned}\dot{\Psi}_{\mathbf{R}}(t)&=\omega_0-J\sin[\Psi_{\mathbf{R}}(t)-\Psi_{\mathbf{R}'}(t-t_D)] \;,\\ \dot{\Psi}_{\mathbf{R}'}(t)&=\omega_0-J\sin[\Psi_{\mathbf{R}'}(t)-\Psi_{\mathbf{R}}(t-\tau_D)] \;,\end{aligned} \tag{6.1}$$

where $\Psi_{\mathbf{R}}$ and $\Psi_{\mathbf{R}'}$ are the average phases of the clusters at locations $\mathbf{R}$ and $\mathbf{R}'$, respectively, τ_D represents the average propagation delay time between pairs of neurons in the two clusters, $J\equiv J_{\mathbf{RR}'}$, and we have neglected noise. The above equations describing a pair of phase oscillators with a delayed interactions is a special case of the model studied by Schuster and Wagner,[33] where different driving frequencies for the two oscillators were included.

Assuming a solution of the form $\Psi_{\mathbf{R}}(t)=\omega t+\alpha/2$, and $\Psi_{\mathbf{R}'}(t)=\omega t-\alpha/2$, the equation for the frequency of the system is

$$\omega=\omega_0-J\cos\alpha\,\sin\omega\tau_D \;. \tag{6.2}$$

The phase shift α can be either 0 or π. A linear stability shows that the above solutions are stable if and only if they obey

$$\alpha=\begin{cases}0, & \cos\omega\tau_D>0\\ \pi, & \cos\omega\tau_D<0\;.\end{cases} \tag{6.3}$$

The low-frequency branches and their stability for $\tau_D=1/\omega_0$ and $2/\omega_0$ are shown in Fig. 14.

The above results imply that synchronized states with zero phase shifts are stable only if the propagation delay obeys $0<\tau_D<\pi/2\omega$. More generally,

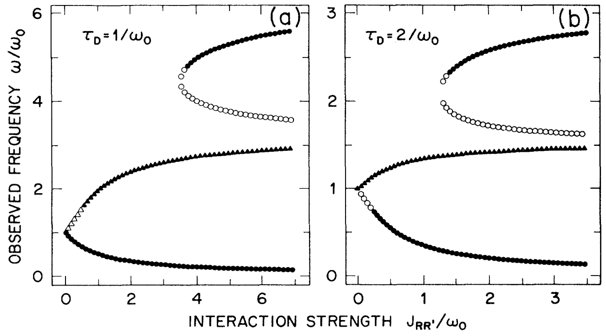

FIG. 14. The true frequency ω of two clusters whose interaction $J_{\mathrm{RR}'}$ is delayed by a propagation time τ_D [(6.1)]. The driving frequency of each cluster is ω_0. Solid symbols correspond to stable solutions of the dynamic equations and open symbols correspond to unstable solutions [(6.2)]. Circles correspond to solutions with zero phase shift, i.e., $\alpha=0$, and triangles correspond to those with a phase shift $\alpha=\pi$ [(6.3)]. (a) A time delay of $\tau_D=1/\omega_0$. The delay is less than $(\pi/2)/\omega$ and thus for small values of $J_{\mathrm{RR}'}$ there are no phase shifts associated with the stable solution [(6.3)]. (b) A time delay of $\tau_D=2/\omega_0$. For small values of $J_{\mathrm{RR}'}$ there is a phase shift of π associated with the stable solution [(6.3)].

$$\frac{(4n-1)\pi}{2\omega}<\tau_D<\frac{(4n+1)\pi}{2\omega}, \quad n=0,1,2,3,\ldots \tag{6.4}$$

It is important to note that the bounds on τ_D are in terms of the true frequency of the system ω and not in terms of the driving frequency ω_0. For the case of the oscillations in the visual cortex, these results imply that the synchronization between neurons is not disrupted for $\tau_D < \sim 6$ ms. This bound corresponds to a propagation delay between neurons that are separated by roughly 5 mm.

As noted in Ref. 33 and shown in Fig. 14, increasing the value of J leads to the appearance of multiple, stable solutions with different frequencies and phase shifts. Numerical simulations of (6.1) indicates that each of the two stable low-frequency branches have a substantial basin of attraction. In our model, however, the coupling $J_{\mathrm{RR}'}$ is weak, i.e., of order ϵ [(4.30)], and there is only one stable solution for a given value of τ_D (Fig. 14).

VII. DIRECTIONAL SELECTIVITY

We have considered so far neurons that are sensitive only to the orientation of the stimulus (Fig. 2). For these cells, there is no difference between an oriented bar that moves forward along a fixed axis and one that moves backward along the same axis. It is well known,[28,34] however, that neurons may be sensitive to the direction as well as the orientation of a moving bar. We now consider an architecture in which a fraction of the cells in each cluster encode direction as well as orientation. Motivated by experimental evidence[6] and computational considerations, we seek an effective interaction between clusters that allows their phases to remain uncorrelated when bars with similar orientation move in opposite directions through their respective receptive fields.

To incorporate both direction and orientation, we define the tuning curves on the interval from 0 to 2π rather than from 0 to π. Neurons that encode both direction and orientation have a single peak in their tuning curve. In contrast, neurons that encode only orientation have two peaks in their tuning curve, at θ and $\theta+\pi$. For simplicity, the double-peaked tuning curves are described as the sum of the tuning curves of two directional sensitive cells, one peaked at θ and the other at $\theta+\pi$.

There are three sets of long-range connections that may exist in this system. One corresponds to the connections between cells that are orientation selective but are insensitive to directions, i.e., $F_L(\theta-\theta')$ [(2.7)], and has a periodicity of π. A second, designated $F'_L(\theta-\theta')$, describes the connections between cells that are sensitive to direction and has a periodicity of 2π. A third type describes the connections between neurons that are sensitive to direction and those that are not. These connections are taken to be zero, a simplification that will not effect the essence of our conclusions.

We consider the effective interaction for two experimental paradigms (Fig. 15). The first involves *stationary*, oriented stimuli, such as flashing bars, that stimulate neurons in different clusters. The most general form of the effective interaction for this paradigm, denoted $J^{\mathrm{stat}}_{\mathrm{RR}'}$, is

$$J^{\mathrm{stat}}_{\mathrm{RR}'}=W_L\frac{1}{(2\pi)^2}\int_0^{2\pi}\int_0^{2\pi}d\theta\, d\theta'\; V_{\mathrm{R}}(\theta)\{a_1F_L(\theta-\theta')+a_2[F'_L(\theta-\theta')+F'_L(\theta-\theta'+\pi)]\}V_{\mathrm{R}'}(\theta') , \tag{7.1}$$

where a_1 and a_2 are positive constants [Fig. 15(a)]. The interaction $J^{\mathrm{stat}}_{\mathrm{RR}'}$ has a period of π, as required for stationary stimuli.

The second paradigm involves *moving* stimuli. The most general form of the effective interaction for this case, denoted $J^{\mathrm{move}}_{\mathrm{RR}'}$, is

$$J^{\mathrm{move}}_{\mathrm{RR}'}=W_L\frac{1}{(2\pi)^2}\int_0^{2\pi}\int_0^{2\pi}d\theta\, d\theta' V_{\mathrm{R}}(\theta)[a_3F_L(\theta-\theta')+a_4F'_L(\theta-\theta')]V_{\mathrm{R}'}(\theta') \tag{7.2}$$

where a_3 and a_4 are constants [Figs. 15(a) and 15(b)]. The interaction $J^{\mathrm{move}}_{\mathrm{RR}'}$ has a period 2π, as required. However, the contribution from $F_L(\theta-\theta')$ has periodicity π. Thus if $F_L(\theta-\theta')$ has a maximum at $\theta-\theta'=0$, its contribution to $J^{\mathrm{move}}_{\mathrm{RR}'}$ will result in a maximum in $J^{\mathrm{move}}_{\mathrm{RR}'}$ for both $\Delta\theta_0=0$ and π. This will tend to synchronize clusters when the bars move in opposite directions through their respective receptive fields. To counter this effect, the contribution from $F_L'(\theta-\theta')$ must be negative near $\theta-\theta'=\pi$ [Fig. 15(c)].

We conclude quite generally that the ability to discriminate between two stimuli with the same orientation, but moving in different directions, places specific constraints on the long-range connectivity. The constraints imposed by orientation discrimination require that neurons insensitive to direction interact with neurons that have the same orientation preference via excitatory connections. As a consequence, the connections between neurons that are sensitive to direction must be inhibitory for neurons with similar orientation preference but opposite directional preference. A more restrictive scheme than the present one, considered previously[26,27] (see also Ref. 21), is to assume that only neurons that encode both direction and orientation mediate the long-range interactions. In that scheme there is no need to include inhibition between neurons with opposite directional preference.

VIII. CODING OF FEATURES BY FREQUENCY

Our model consists of oscillators with identical driving frequencies (2.4). Information about local features is encoded in the connection strengths. This assumption is natural for orientation coded stimulus. It is unlikely that the properties of an active cluster, e.g., the frequency of oscillation, will depend systematically on the orientation of its stimulus since the system is, at least approximately, invariant under rotation of the stimulus.

Similar considerations should hold for encoding the spatial location or direction of motion or a stimulus. On

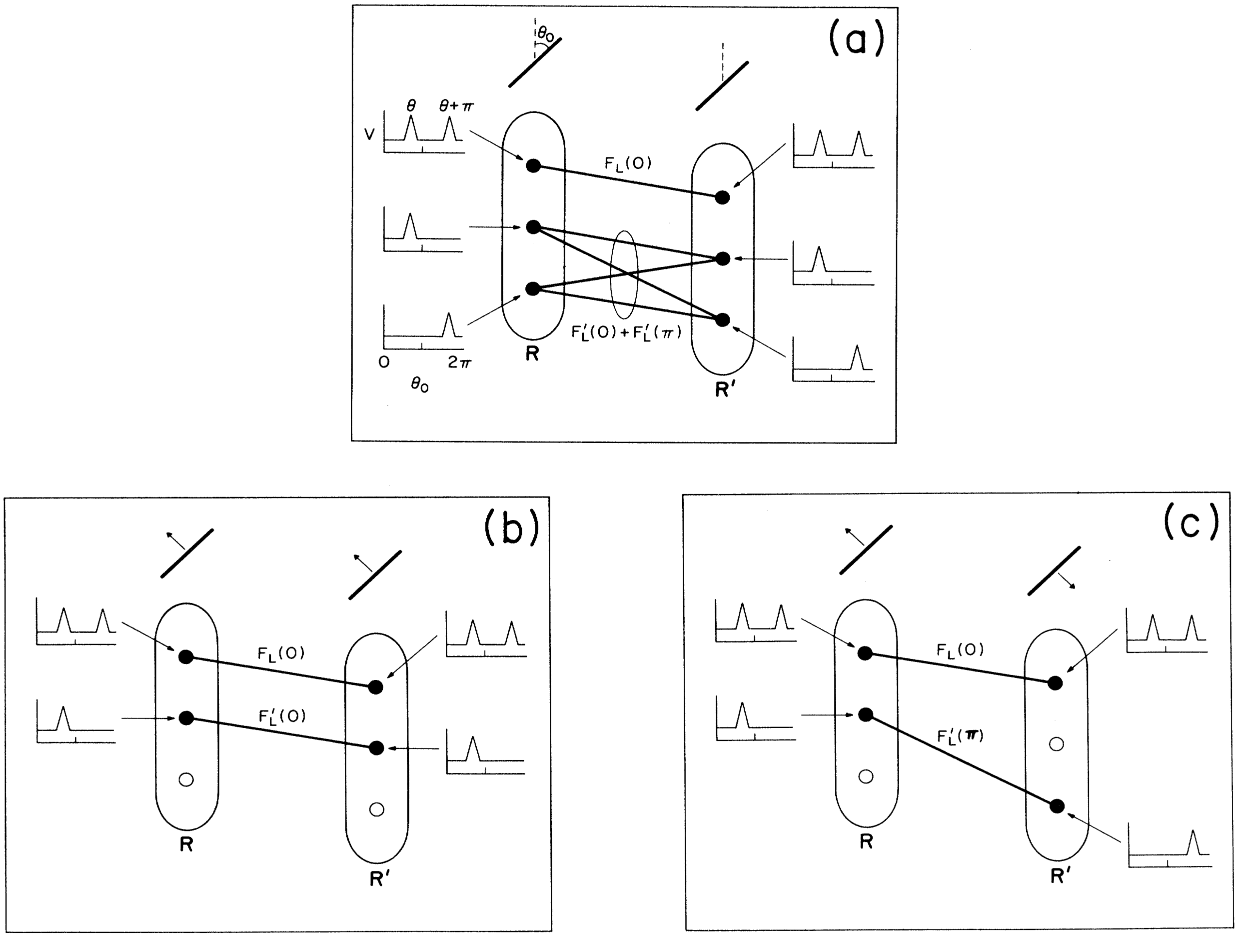

FIG. 15. An architecture that incorporates neurons that are insensitive to the direction of motion of a bar, as well as those that are sensitive to the direction of movement. The directionally insensitive neurons interact via a pattern of connectivity $F_L(\theta-\theta')$, while the directionally sensitive neurons interact via a pattern $F_L'(\theta-\theta')$. (a) The case of stationary, e.g., flashing bars with orientation θ_0. The directionally insensitive neurons as well as neurons sensitive bars moving in either the up or down direction are activated. (b) The case of both bars moving in the same direction. The directionally insensitive neurons in both clusters are activated, but only directionally sensitive neurons that respond to bars moving upward are activated. (c) The case of both bars moving in the opposite direction. The directionally insensitive neurons in both clusters are activated. However, only directionally sensitive neurons that respond to bars moving downward are activated in the **R**th cluster, while only directionally sensitive neurons that respond to bars moving downward are activated in the **R**'th cluster. This schematic shows that $F_L'(\pi)$ must be negative to prevent phase coherence between the two clusters.

the other hand, such symmetries do not exist for the coding of other features, such as stimulus velocity, spatial frequency, or color. It is thus plausible that there is a systematic dependence of local properties, in particular the local driving frequency, on these features. Indeed, there is experimental evidence of a substantial increase in the frequency of oscillations in the cat visual cortex with an increase in the velocity of a moving bar stimulus.[4,8] Such a dependence may provide a complementary mechanism of discriminating between disparate features by the temporal coherence of the neural response.

To examine the implications of a systematic variation of frequency with stimulus properties, let us assume that a single moving bar generates an oscillatory response in a cluster with a frequency that depends on the velocity of the bar. When two bars that move with different velocities are present, the dynamics of the two stimulated clusters can be described by equations similar to (5.1), i.e.,

$$\begin{aligned}\dot{\Psi}_{\mathrm{R}}(t)&=\omega_{\mathrm{R}}-J\sin[\Psi_{\mathrm{R}}(t)-\Psi_{\mathrm{R}'}(t)]\ ,\\ \dot{\Psi}_{\mathrm{R}'}(t)&=\omega_{\mathrm{R}'}-J\sin[\Psi_{\mathrm{R}'}(t)-\Psi_{\mathrm{R}}(t)]\ ,\end{aligned} \tag{8.1}$$

where, as before, Ψ_{R} and $\Psi_{\mathrm{R}'}$ are the average phases of the two clusters. The local driving frequencies ω_{R} and $\omega_{\mathrm{R}'}$ correspond to the driving frequencies for each cluster in the absence of a stimulus in the other receptive field in other cluster. Equations of this form have been studied.[24,35] Denoting $\Psi_{\pm}\equiv\Psi_{\mathrm{R}}\pm\Psi_{\mathrm{R}'}$ and $\omega_{\pm}\equiv\omega_{\mathrm{R}}\pm\omega_{\mathrm{R}'}$, one obtains

$$\dot{\Psi}_{+}=\omega_{+}\ , \tag{8.2a}$$

$$\dot{\Psi}_{-}=\omega_{-}-2J\sin\Psi_{-}\ . \tag{8.2b}$$

The behavior of the system depends on the strength of J relative to ω_{-}.

Small frequency difference: $|2J/\omega_{-}|>1$. In this regime, the solution to (8.2b) is constant in time, i.e.,

$$\Psi_{-}^{0}=\sin^{-1}\left[\frac{\omega_{-}}{2J}\right]\ . \tag{8.3}$$

The phases of the two clusters are locked with a fixed difference in their phase. Evaluating the cross-correlation function of the two phases, one obtains

$$\begin{aligned}C_{\mathrm{RR}'}(\tau)&=\langle\cos[\Psi_{\mathrm{R}}(t+\tau)-\Psi_{\mathrm{R}'}(t)]\rangle\\ &=\cos(\tfrac{1}{2}\omega_{+}\tau+\Psi_{-}^{0})\ .\end{aligned} \tag{8.4}$$

Large frequency difference: $|2J/\omega_{-}|<1$. In this regime the solution of (8.2b) is a periodic function of time, i.e.,

$$\Psi_{-}(t)=2\tan^{-1}\left[\frac{\Omega}{\omega_{-}}\tan(\tfrac{1}{2}\Omega t)+\frac{2J}{\omega_{-}}\right]\ , \tag{8.5}$$

with

$$\Omega=(\omega_{-}^{2}-4J^{2})^{1/2}\ . \tag{8.6}$$

The system undergoes a quasiperiodic motion, with frequencies $\omega_{+}/2$ and Ω. The cross-correlation function of the two phases Ψ_{R} and $\Psi_{\mathrm{R}'}$ has the form

$$C_{\mathrm{RR}'}(\tau)=A(\Omega\tau)\cos[\tfrac{1}{2}\omega_{+}\tau+\chi(\Omega\tau)]\ , \tag{8.7}$$

where both the amplitude A and the phase χ are periodic functions of their arguments, with period 2π.

The above analysis [(8.4) and (8.7)] shows that the induction of a frequency difference between two clusters will affect the magnitude of the correlation and, more importantly, its time dependence. In principle, this change can be used to discriminate between stimuli with disparate local features, e.g., two objects moving with different velocities. Whether this mechanism is actually used by the nervous system remains to be seen. An interesting experiment would be to measure the oscillatory output of neurons that are simultaneously stimulated by bars moving with different velocities. Our analysis suggests that a break of the phase coherence, accompanied by an appearance of a modulation frequency, will develop as the difference in the velocity of the two stimuli is increased. Since the driving frequencies of each cluster can be measured by stimulation with a single bar, these measurements can lead to an estimate of the effective interaction $J_{\mathrm{RR}'}$ between oscillating clusters.

In addition to systematic effects, random variation in the driving frequency of each neuron may be present. This variation may serve as an additional, potential source of noise. Networks of coupled oscillators with a distribution of driving frequencies will remain coherently active provided that the width of this distribution is small relative to the strength of the interactions within a cluster,[24] i.e., $|\delta\omega|\lesssim 1/\tau_{S}$ [(4.25)].

IX. DISCUSSION

We have presented a phenomenological model of segmentation of visual scenes by a network of oscillatory neurons. The dynamics of each neuron is described by a phase variable. This description does not consider the origin of the oscillations and oversimplifies the neuronal dynamics. Nevertheless, such an approach is justified at present, given the lack of experimental guidance on the neuronal circuitry that generates and modulates the observed oscillations. Our phenomenological model provides a framework that defines the minimal requirements to realize a neuronal circuit that generates coherent activity similar to that observed in the cat visual cortex.[4-8] Furthermore, it specifies how these oscillations can be used to link and segment stimuli that span multiple receptive fields.

An advantage of our phenomenological approach is that the description of the temporal and spatial coherence in the neurons involves few parameters, e.g., the scales of short-range and long-range connection strength and the level of noise. These parameters can, in principle, be determined from the amplitude and time dependence of the measured correlation functions. Furthermore, there are predicted relationships among the correlation functions [(4.27) and (4.33)]. An additional advantage of our approach is that it provides a means to compare different models of visual processing that incorporate a microscopic description of the underlying neuronal circuitry. Under appropriate conditions, such detailed models may reduce to a phase description, with the effective scales of connection strength and noise expressed in terms of the underlying microscopic variables. Finally, the phase description provides a convenient computational model that can be tested against other schemes for global visual tasks.

A. Assumptions that underly the model

1. Architecture of connectivity

Our model assumed that neurons that share the same receptive field are grouped in clusters. The interactions between neurons within clusters are strong and depend only moderately on the orientation preference of the neurons. The interactions between neurons in different clusters are relatively weak and depend critically on their orientation preference.

This architecture offers a number of attractive computational features, some of which have been alluded to above (Figs. 10–13). Quite generally, this architecture allows proximal stimuli with disparate features to be linked as a single object. Consider, for example, the recognition of the connected versus the disconnected pattern in Fig. 16. For the connected pattern, the neurons that respond to orthogonal segments interact via short-range connections. Thus the output of all of the neurons oscillates coherently. For the disconnected pattern, the neurons that respond to orthogonal segments do not interact. Thus their output is segmented into two coherent populations. In addition, the architecture in our model may provide a mechanism for linking several features, e.g., orientation and color, that are processed by different neurons that share the same receptive field.

The notion that the specificity of cortical connections depends on the orientation preference of cells is supported by physiological and anatomical data.[36,37] The majority of the evidence indicates that there are excitatory interactions between cells with similar preferences. Furthermore, there are claims of inhibitory interactions between cells with different orientation preferences.[38–40]

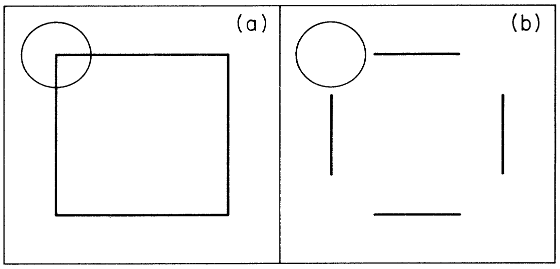

FIG. 16. Patterns formed from orthogonal lines. (a) A continuous pattern. (b) A discontinuous pattern. The circles correspond to the assumed upper bound on the size of a receptive field. Within the framework of our model, the neurons that respond to the continuous pattern are fully synchronized, while those that respond to the discontinuous object are segmented into two populations.

The relative nonspecificity of the short-range interaction assumed in our model is supported by the relative insensitivity of the coherence of proximal neurons to their orientational preference.[4,6,7] However, other physiological data on orientation specificity of connections does not reveal a clear difference between short-range and long-range connections.[36] Furthermore, there are recent indications that the coherence of the oscillations of proximal neurons, stimulated by two moving bars, is sensitive to the relative orientation of the bars.[41] This important issue deserves further experimental and theoretical study.

2. Activity-dependent connections and discrimination

In order to achieve dependence of the coherence between the phases of a pair of neurons phases on the orientation of their respective stimuli, the coupling between the phases must depend on their levels of activity. We have modeled this dependence in a Hebb-like manner (2.4). However, the levels of activity, as represented by the tuning curves, are typically relatively broad. Our analysis implies that a simple linear dependence of the connections on each activity level, i.e., $V(\mathbf{r}) \simeq \Gamma(\mathbf{r})$ [(2.5)], leads to relatively poor and computationally uninteresting discrimination for the case of purely excitatory connections (Appendix A). In the present work, we achieve an enhanced discrimination by adopting a highly nonlinear dependence of the connections on the average local levels of activity. The particular nonlinearity we chose was a threshold function, so that only neurons whose activity is above a minimum, substantial value can contribute to the interaction [(3.14)]. An alternate possibility is to assume that the interactions depend on a power of the local activity, e.g., $J(\mathbf{r},\mathbf{r}') = \Gamma^n(\mathbf{r}) W(\mathbf{r},\mathbf{r}') \Gamma^n(\mathbf{r}')$ with $n > 1$. The nonlinearities for either scheme can, in principle, be mediated by interneurons.

A sharp angular dependence of the effective interaction between neurons in different clusters can also be achieved when the interactions between neuronal phases have a *linear* dependence on the average levels of local activities. This requires the use of inhibitory as well as excitatory long-range connections.[26,27] The exact form of the dependence of the long-range connections on the orientation preference of the neurons is a sensitive function of the shape of the tuning curve (Appendix A). A sophisticated model may combine both inhibitory connections and nonlinear schemes.[42]

The required activity dependence is suggestive of a fast, Hebb-like modification of the strength of the underlying synaptic connections.[1,43] A *possible* biophysical basis for these fast changes are excitatory synaptic currents that are mediated by *n*-methyl-*D*-aspartate (NMDA) receptors.[2] Indeed, there are recent experimental findings that suggest that NMDA receptors mediate a significant fraction of the synaptic currents in the primary visual cortex.[44] Hebb-like activity dependence may also reflect a modulation of interactions by appropriate circuits of interneurons.

The results of recent studies[10,14,17] suggest that activity-dependent coupling between phases may emerge as a consequence of the interactions among neuronal oscillators in which both amplitudes and phases are dynamic variables. In such a network, the coupling between the phase of the neuronal oscillations will depend on activity of the neurons even when the underlying synaptic interactions have a fixed strength. This dynamic effect may, in principle, account for the required dependence of the phase coherence on the activity of the pre- and postsynaptic cell. Indeed, a preliminary analysis of this effect using a model of analog neurons suggests that the synchronization of a pair of oscillatory neurons depends strongly on their levels of activity.[27] This important issue is currently under study.

3. Transient behavior

The usefulness of a network for the discrimination of stimuli that evolve in time depends on the transient behavior of the network. A particularly important element is the time necessary for correlations between the output of different clusters to form or to decay as the stimulus changes. Roughly, this time should not exceed a few times the period of oscillations. Indeed, the experimental evidence suggests that the correlations are formed within at most a few periods.[45,46]

The architecture employed in our model assumes that the synchronizing, long-range connections between different clusters are weak. The advantage of this scaling is that the local coherence is relatively insensitive to the global properties of the stimulus. On the other hand, the time to establish synchronization between spatially separate regions can be quite long with weak long-range connections. Specifically, the time required to establish substantial correlations among different clusters scales as $\tau_L \sim 1/W_L$, which can be significantly longer than the time required for the onset of coherent output within each cluster, i.e., $\tau_S \sim 1/W_S$ [(4.25)]. The time for the output of different clusters to dephase following a drop in the strength of their effective interaction is governed by the level of the correlated noise. This noise scales as $1/T_L \sim 1/W_L$ and thus the dephasing time is also on the order of τ_L.

B. Relation to our earlier work

In the present work we extend our original model[26,27] in a number of ways that significantly improve its computational effectiveness. One issue involves the necessity for the correlation between clusters to respond rapidly to changes in the orientation of the stimuli. The response time depends on the time required for the output of two clusters to dephase (see above), which is set by the residual noise in a cluster. In our original formulation, the residual noise level resulted from the presence of a finite number of active neuronal oscillators in each cluster, each with an independent, local noise. The level of this residual noise is approximately T_S/N, where T_S is the variance of the local noise and N is the number of neurons in a cluster. It can be very low when the number of neurons is large. In the present work, we include an additional source of noise, correlated across a cluster, so that the residual noise level is an independent parameter. The two scales of noise in the present network, localized noise and relatively weak correlated noise [(2.8)], are analogous to the two scales of connection strength [(2.12)]. We suggest that it is reasonable for the noise to have a component that is correlated on the length scale of the local connectivity, roughly equivalent to that of a hypercolumn in the visual cortex.

A second issue involves the ability of the network to discriminate between short bars with different orientation, each in a separate receptive field. The sharpness of this discrimination depends on the form of the effective interaction between pairs of clusters. In our original work we assumed that the effective interaction was *linearly* mediated by the firing rate of each neuron and used a pattern of long-range connectivity that consisted of inhibitory as well as excitatory interactions. Although this scheme allows the network to achieve sharp discrimination (Fig. 4), we observed numerically that it is overly sensitive to the shape of the tuning curve as well as to small variations in the form of the long-range connections. Here we adopted an alternate, robust scheme in which the effective interaction between neuronal phases is mediated by a *nonlinear* function of the rate of firing (Fig. 5).

A final issue concerns the discrimination between bars that move with the same orientation but in different directions. Previously, we considered a particular scheme for the pattern of connectivity in which only neurons sensitive to direction as well as orientation mediate the long-range interactions. In the present work we consider a general formulation of the problem, in which the connections that mediate discrimination by the direction of movement are decoupled from those that mediate discrimination based on orientation. In this scheme the connections between neurons that are sensitive to direction must be inhibitory for neurons with similar orientation preference but opposite directional preference (Fig. 15). More generally, it is well known that visual stimuli are coded for a multitude of features, e.g., spatial frequency and color, in addition to orientation.[28] Our analysis suggests how the long-range connections can cause phase coherence to be unfavorable when there is discordance in any feature between neighboring stimuli (see also Ref. 21).

C. The issue of read-out

An important issue is the time required to make a discrimination on the basis of the correlation among the neuronal phases. In the presence of noise, determination of these correlations necessitates the need to temporally average the output from different clusters. The details of this averaging will depend on the assumed scheme to "read-out" the correlations, an open question at the present time. Qualitatively, the time required for averaging will be determined largely by the ratio of the long-range interactions to the correlated noise, i.e., W_L/T_L. This ratio can, in principle, be estimated from the equilibrium value of $C_{\mathrm{RR}'}(0)$.

D. Extension to other features

We have presented a detailed model of processing of orientation-coded stimuli. Recognition of complex visual stimuli requires the processing of several features. Our model may provide a framework for such processing. Local interactions may link different features within a receptive field. Processing of sensory input across many fields will be mediated by the dependence of long-range interactions and local frequencies on the stimulus. Accomplishing this goal may require the incorporation of more biologically realistic[47] and computationally powerful[48] neuronal receptive fields.

ACKNOWLEDGMENTS

We thank J. M. Bower, C. Koch, H. G. Schuster, T. B. Schillen, T. J. Sejnowski, and O. Sporns for sending us copies of their work prior to publication. We thank F. H. C. Crick, C. M. Gray, P. C. Hohenberg, P. Konig, C. v. d. Malsburg, R. Meir, W. Singer, and R. A. Stepnoski for useful discussions. D.K. and H.S. thank the Aspen Center for Physics for its hospitality. This work was supported, in part, by the Fund for Basic Research administered by the Israeli Academy of Arts and Sciences and by the U.S.–Israel Binational Science Foundation.

APPENDIX A: LINEAR MECHANISM FOR A SHARP $J_{\mathbf{RR}'}$

The strength of the effective interaction $J_{\mathbf{RR}'}$ is a function of the difference in the orientation of stimuli between two clusters $\Delta\theta_0$. The sharpness of the interaction depends on the functional relationship between $V_{\mathbf{R}}(\theta)$ and $\Gamma_{\mathbf{R}}(\theta)$ and on the form of long-range connectivity $F_L(\theta-\theta')$. In the text, we focused on $V_{\mathbf{R}}(\theta)$ that were thresholded versions of the tuning curves, so that $V_{\mathbf{R}}(\theta)=0$ for $|\theta|>\sigma$. Here, as in our previous work,[26,27] we consider in detail the case of $V_{\mathbf{R}}(\theta)$ that are nonzero for all orientations.

The linear relation between $J_{\mathbf{RR}'}(\Delta\theta_0)$ and $F_L(\theta-\theta')$ can be cast into a convenient form by Fourier transforming (3.1). Denoting the transforms of $J_{\mathbf{RR}'}(\Delta\theta_0)$, $F_L(\theta)$ and $V(\theta)$ by $\tilde{J}_{\mathbf{RR}'}(l), \tilde{F}_L(l)$, and $\tilde{V}_L(l)$, respectively, yields

$$\tilde{J}_{\mathbf{RR}'}(l)=W_L|\tilde{V}(l)|^2\tilde{F}_L(l)\ . \tag{A1}$$

For concreteness, we take an exponential form for $V_{\mathbf{R}}(\theta)$ [(3.7)], i.e.,

$$V_{\mathbf{R}}(\theta)=e^{-|\theta_0(\mathbf{R})-\theta(\mathbf{R})|/\kappa}\ , \tag{A2}$$

where κ is the width of the tuning curve. We consider first the possibility that the long-range connections are purely excitatory and occur only between neurons with similar orientation preferences, i.e., $F_L(\theta-\theta')=\kappa\delta(\theta-\theta')$. This hypothesis leads to

$$J_{\mathbf{RR}'}(\Delta\theta_0)\simeq W_L\left[1+\frac{|\Delta\theta_0|}{\kappa}\right]e^{-|\Delta\theta_0|/\kappa}\ . \tag{A3}$$

The resultant orientation dependence is relatively weak. The angular range of this interaction is roughly twice the width of the neuronal tuning curve [Fig. 4(b)].

Within the framework of a linear relationship between $V_{\mathbf{R}}(\theta)$ and $\Gamma_{\mathbf{R}}(\theta)$, a sharp dependence of $J_{\mathbf{RR}'}$ on $\Delta\theta_0$ for forms of $V_{\mathbf{R}}(\theta)$ that decay smoothly to zero requires the use of inhibitory as well as excitatory long-range connections. For the exponential form of $V_{\mathbf{R}}(\theta)$ [(A2)], an interesting form of such connectivity is

$$\begin{aligned} F_L(\theta-\theta') &= \left[1-\left[\frac{\kappa}{\rho}\right]^2\frac{\partial^2}{\partial x^2}\right]^2 e^{-x^2/2} \\ &= \left[1-2\left[\frac{\kappa}{\rho}\right]^2(x^2-1)\right. \\ &\qquad \left.+\left[\frac{\kappa}{\rho}\right]^4(x^4-6x^2+3)\right]e^{-x^2/2}\ , \end{aligned} \tag{A4}$$

where $x\equiv(\theta-\theta')/\rho$ and ρ is a free parameter that controls the angular range of the effective interaction. A reasonable choice for this parameter is $\rho\leq\kappa$. The effective interaction, found from (A1), is

$$J_{\mathbf{RR}'}\simeq W_L e^{-(\Delta\theta_0)^2/2\rho^2}\ . \tag{A5}$$

For $F_L(\theta-\theta')$ with $\rho=0.4\kappa$, the range of $J_{\mathbf{RR}'}$ is about 0.5κ.

APPENDIX B: TIME DEPENDENCE OF THE AUTOCORRELATION FUNCTIONS

The autocorrelation function $C_{\mathbf{R}}(\theta,\tau)$ can be calculated analytically for two limiting cases of the local noise level T_S. These are (i) at high levels of noise, i.e., $T_S>T_C$, where the order parameter $M=0$ and the equation for noisy components of the phases [(4.22)] reduce to

$$\delta\dot{\phi}_{\mathbf{R}}(\theta,t)=\zeta_{\mathbf{R}}(\theta,t)\ ; \tag{B1}$$

and (ii) at low noise levels, where $\delta\phi_{\mathbf{R}}(\theta,t)$ is small and (4.22) can be linearized, i.e.,

$$\delta\dot{\phi}_{\mathbf{R}}(\theta,t)=\zeta_{\mathbf{R}}(\theta,t)-\frac{1}{\tau_S}\delta\phi_{\mathbf{R}}(\theta,t)\ , \tag{B2}$$

where τ_S is defined in (4.25).

The autocorrelation function is (4.21)

$$C_{\mathbf{R}}(\theta,\tau)=\langle\cos z\rangle\ , \tag{B3}$$

where

$$z\equiv\phi_{\mathbf{R}}(\theta,t)-\phi_{\mathbf{R}}(\theta,t+\tau)\ . \tag{B4}$$

For both limiting noise levels, z is a Gaussian variable with zero mean and variance Δ^2. At high noise levels

$$z=\int_0^\tau dt'\zeta_{\mathbf{R}}(\theta,t') \tag{B5}$$

and

$$\Delta^2=2|\tau|T_S\ . \tag{B6}$$

At low levels of noise and for large averaging times

$$z=\int_{-\infty}^{0}dt'\zeta_{\mathbf{R}}(\theta,t')e^{t'/\tau_S}-\int_{-\infty}^{\tau}dt'\zeta_{\mathbf{R}}(\theta,t')e^{(t'-\tau)/\tau_S} \tag{B7}$$

and

$$\Delta^2=2\tau_S T_S(1-e^{|\tau|/\tau_S}) \ . \tag{B8}$$

The autocorrelation function is calculated by Gaussian integration, i.e.,

$$C_{\mathbf{R}}(\theta,\tau)=\int_{-\infty}^{\infty}dz\frac{e^{-z^2/2\Delta^2}}{(2\pi\Delta^2)^{1/2}}\cos z=e^{-\Delta/2} \ . \tag{B9}$$

Substituting (B6) yields, for high levels of noise,

$$C_{\mathbf{R}}(\theta,\tau)=e^{-|\tau|T_S} \ . \tag{B10}$$

Substituting (B6) yields, for low levels of noise,

$$C_{\mathbf{R}}(\theta,\tau)=e^{-\tau_S T_S(1-e^{-|\tau|/\tau_S})} \ . \tag{B11}$$

The mean-field result for $C_{\mathbf{R}}(\theta,t)$ [(4.21)] and the long-time limit of (B11) imply

$$m_{\mathbf{R}}^2(\theta)=e^{-\tau_S T_S} \ . \tag{B12}$$

When $T_S\tau_S \ll 1$, (B11) can be approximated by

$$\begin{aligned}C_{\mathbf{R}}(\theta,\tau)&\simeq 1-\tau_S T_S(1-e^{-|\tau|/\tau_S})\\&\simeq[1-m_{\mathbf{R}}^2(\theta)]e^{-|\tau|/\tau_S}+m_{\mathbf{R}}^2(\theta) \ .\end{aligned} \tag{B13}$$

The above equation is a useful approximation for $C_{\mathbf{R}}(\theta,\tau)$ even if the linear approximation [(B2)] is not valid, so long as $m_{\mathbf{R}}(\theta)$ is not small.

APPENDIX C: CORRELATION FUNCTION FOR A LONG BAR

We calculate the intercluster cross-correlation function for the case of a straight bar that spans K receptive fields and is described by the energy function given by (5.4). It is useful to define the two-dimensional unit-length vectors

$$\vec{S}_R=(\cos\psi_R,\sin\psi_R) \tag{C1}$$

in order to evaluate the equilibrium properties of the system of phases with this energy [(5.4)]. Up to a constant, irrelevant term, the energy can be written as

$$E=-\frac{W_L}{2}\|\vec{S}\|^2 \ , \tag{C2}$$

where $\vec{S}\equiv\sum_{\mathbf{R}=1}^{K}\vec{S}_{\mathbf{R}}$.

The partition function of the system is

$$Z=\int\prod_{\mathbf{R}}^{K}d\vec{S}_{\mathbf{R}}e^{1/2\beta_L W_L\|\vec{S}\|^2} \tag{C3}$$

where the integration over $d\vec{S}_{\mathbf{R}}$ is restricted to the unit circle. Using the well-known Hubbard-Strantonovitch transformation, we obtain

$$Z=\frac{1}{2\pi}\int_{-\infty}^{\infty}d\vec{X}e^{-1/2\vec{X}^2}\int\prod_{\mathbf{R}}^{K}d\vec{S}_{\mathbf{R}}e^{(\beta_L W_L)^{1/2}\vec{X}\cdot\vec{S}} \ , \tag{C4}$$

where $\vec{X}$ is a two-dimensional variable. Using polar coordinates (x,θ) for $\vec{X}$, (C4) reduces to an integral over a single variable, i.e.,

$$Z=\int_{0}^{\infty}x\,dx\,e^{-1/2x^2+K\ln\mathcal{J}_0((\beta_L W_L)^{1/2}x)} \ , \tag{C5}$$

where $\mathcal{J}_0(x)$ is the zeroth-order modified Bessel function.

The average value of the energy $\langle E\rangle$ can be calculated from (C5) by the standard relation

$$\langle E\rangle=-\frac{\partial\ln Z}{\partial\beta_L} \ . \tag{C6}$$

Using (C2), one can write the average value as

$$\langle E\rangle=-\frac{W_L}{2}[K(K-1)C_{\mathbf{RR}'}+K] \ , \tag{C7}$$

where the equivalence of all of the pairwise correlations in this system has been employed. Using (C6) and (C7), we find

$$C_{\mathbf{RR}'}=\frac{1}{K-1}\left[\frac{1}{(\beta_L W_L)^{1/2}}\langle x\mathcal{H}((\beta_L W_L)^{1/2}x)\rangle-1\right] \ , \tag{C8}$$

where

$$\langle f(x)\rangle\equiv\frac{1}{Z}\int_{0}^{\infty}dx\,xf(x)e^{-1/2x^2+K\ln\mathcal{J}_0((\beta_L W_L)^{1/2}x)} \ , \tag{C9}$$

and $\mathcal{H}(x)=\mathcal{J}_1(x)/\mathcal{J}_0(x)$, where $\mathcal{J}_1(x)$ is the first-order modified Bessel function. Equations (C8) and (C9) can be evaluated numerically to yield $C_{\mathbf{RR}'}$ for all values of the parameters β_L, W_L, and K.

---

[*] Permanent address.

[†] Author to whom reprint request can be made at Room 1C-463, AT&T Bell Laboratories, 600 Mountain Avenue, Murray Hill, NJ 07974.

[1] Ch. von der Malsburg and W. Schneider, Biol. Cybern. **54**, 29 (1986).

[2] C. M. Gray, P. Konig, A. K. Engel, and W. Singer, in *Synergetics of Cognition,* edited by H. Haken and M. Stadler (Springer-Verlag, New York, 1990), pp. 82–98.

[3] F. H. C. Crick and C. Koch, Semin. Neurosci. **2**, 263 (1990).

[4] R. Eckhorn, R. Bauer, W. Jordan, M. Brosch, W. Kruse, M. Munk, and R. J. Reitboeck, Biol. Cybern. **60**, 121 (1988).

[5] C. M. Gray and W. Singer, Proc. Natl. Acad. Sci. U.S.A. **86**, 1698 (1988).

[6] C. M. Gray, P. Konig, A. K. Engel, and W. Singer, Nature **338**, 334 (1989).

[7] A. K. Engel, P. Konig, C. M. Gray, and W. Singer, Eur. J. Neurosci. **2**, 588 (1990).

[8] C. M. Gray, A. K. Engel, P. Konig, and W. Singer, Eur. J. Neurosci. **2**, 607 (1990).

[9] J. Allman, F. Miezin, and E.-Y. McGuinness, Annu. Rev. Neurosci. **8**, 407 (1985).

[10] O. Sporns, J. A. Gally, G. N. Reeke, and G. M. Edelman, Proc. Natl. Acad. Sci. U.S.A. **86**, 7265 (1989).

[11] D. M. Kammen, P. J. Holmes, and C. Koch, in *Models of Brain Function*, edited by R. M. J. Cotterill (Cambridge University Press, London, 1989), pp. 273–284.

[12] R. Eckhorn, R. J. Reitboeck, P. Dicke, M. Arndt, and W. Kruse, in *Parallel Processing in Neural Systems and Computers,* edited by R. Eckmiller, E.. Hartman, and G. Hauske (Elsevier Science, Amsterdam, 1990), pp. 101–104.

[13] T. B. Schillen and P. Konig, in *Parallel Processing in Neural Systems and Computers* (Ref. 12), pp. 139–142.

[14] H. G. Schuster and P. Wagner, in *Parallel Processing in Neural Systems and Computers* (Ref. 12), pp. 143–146.

[15] M. A. Wilson and J. A. Bower, in *Advances in Neural Network Information Processing Systems 2,* edited by D. Touretzky (Kaufmann, San Mateo, 1990), pp. 84–91.

[16] R. Eckhorn, R. J. Reitboeck, M. Arndt, and P. Dicke, Neural Comput. **2**, 293 (1990).

[17] H. G. Schuster and P. Wagner, Biol. Cybern. **64**, 77 (1990).

[18] H. G. Schuster and P. Wagner, Biol. Cybern. **64**, 83 (1990).

[19] P. Baldi and R. Meir, Neural Comput. **2**, 458 (1990).

[20] T. B. Schillen and P. Konig, Neural Comput. (to be published).

[21] P. Konig and T. B. Schillen, Neural Comput. (to be published).

[22] O. Sporns, G. Tononi, and G. M. Edelman, Proc. Natl. Acad. Sci. U.S.A. **88**, 129 (1991).

[23] W. W. Lytton and T. J. Sejnowski (unpublished).

[24] Y. Kuramoto, *Chemical Oscillations, Waves, and Turbulence* (Springer-Verlag, New York, 1984).

[25] N. Kopell and G. B. Ermentrout, Commun. Pure Appl. Math. **39**, 623 (1986).

[26] H. Sompolinsky, D. Golomb, and D. Kleinfeld, Proc. Natl. Acad. Sci. U.S.A. **87**, 7200 (1990).

[27] H. Sompolinsky, D. Golomb, and D. Kleinfeld, in *Nonlinear Dynamics and Neuronal Networks,* edited by H. G. Schuster and W. Singer (VCH, Weinheim, in press).

[28] G. A. Orban, *Neuronal Operations in the Visual Cortex* (Springer-Verlag, New York, 1984).

[29] C. D. Gilbert, Annu. Rev. Neurosci. **6**, 217 (1983).

[30] K. A. C. Martin, in *Cerebral Cortex,* edited by E. G. Jones and A. Peters (Plenum, New York, 1984), Vol. 2, pp. 241–284.

[31] D. H. Perkel, G. L. Gerstein, and G. P. Moore, Biophys. J. **7**, 391 (1967).

[32] D. H. Perkel, G. L. Gerstein, and G. P. Moore, Biophys. J. **7**, 419 (1967).

[33] H. G. Schuster and P. Wagner, Prog. Theor. Phys. **81**, 939 (1989).

[34] J. McLean and L. A. Palmer, Vision Res. **29**, 675 (1989).

[35] S. H. Strogatz and R. E. Mirollo, J. Phys. A **21**, L699 (1988).

[36] D. Y. Ts'o, C. D. Gilbert, and T. N. Wiesel, J. Neurosci. **6**, 1160 (1986).

[37] H. J. Luhmann, J. M. Greuel, and W. Singer, Eur. J. Neurosci. **2**, 369 (1990).

[38] J. A. Matsubara, M. S. Cynader, and N. V. Swindale, J. Neurosci. **7**, 1428 (1987).

[39] Y. Hata, T. Tsumoto, K. Hagihara, and H. Tamura, Nature **335**, 815 (1988).

[40] A. M. Sillito, in *Cerebral Cortex* (Ref. 30), pp. 91–117.

[41] A. K. Engel, P. Konig, C. M. Gray, and W. Singer, in *Parallel Processing in Neural Systems and Computers* (Ref. 12), pp. 105–108.

[42] J. Malik and P. Perona, J. Opt. Soc. Am. **7**, 923 (1990).

[43] Ch. von der Malsburg and E. Bienenstock, in *Disordered Systems and Biological Organization,* edited by E. Bienenstock, F. Fogelman, and G. Weisbuch (Springer-Verlag, Berlin, 1986), pp. 247–272.

[44] K. D. Miller, B. Chapman, and M. P. Stryker, Proc. Natl. Acad. Sci. U.S.A. **86**, 5183 (1989).

[45] C. Gray, A. K. Engle, P. Koenig, and W. Singer, in *Nonlinear Dynamics and Neuronal Networks* (Ref. 27).

[46] R. Eckhorn and R. J. Reitboeck, in *Nonlinear Dynamics and Neuronal Networks* (Ref. 27).

[47] J. P. Jones and L. A. Palmer, J. Neurophys. **58**, 1187 (1987).

[48] J. G. Daughman, J. Opt. Soc. Am. **2**, 1160 (1985).